Macromolecules

ARTICLE

pubs.acs.org/Macromolecules

# Polysiloxanes Bearing Pendant Redox-Active Dendritic Wedges Containing Ferrocenyl and ($\eta^6$-Aryl)tricarbonylchromium Moieties

Magdalena Zamora, Sonia Bruña, Beatriz Alonso, and Isabel Cuadrado*

Departamento de Química Inorgánica, Facultad de Ciencias, Universidad Autónoma de Madrid, Cantoblanco, 29049, Madrid, Spain

Supporting Information

**ABSTRACT:** Novel highly functionalized polysiloxanes have been synthesized, which bear small pendant dendritic wedges containing two different redox-active organometallic moieties, namely the electron-donating ferrocenyl group and the electron withdrawing ($\eta^6$-aryl)tricarbonylchromium entity. Hydrosilylations of vinylsilyl-functionalized ($CH_2$═$CH$)MePhSiFc (**1**) and allylsilyl-terminated dendron ($CH_2$═$CHCH_2$)PhSi[$(CH_2)_2$MePhSiFc]$_2$ (**3**), with the Si−H-containing polysiloxane backbones $(Me_3SiO)(MeSiHO)_n(Me_2SiO)_m(SiMe_3)$ ($n$ = 30−35%, $m$ = 65−70%), and $(Me_3SiO)(MeSiHO)_n(SiMe_3)$ ($n \sim 35$) successfully afforded the novel siloxane-based copolymers **8** and **9** and homopolysiloxanes **10** and **11** possessing appended organometallic dendritic side chains. Thermal treatment of **8** with $Cr(CO)_6$ and reaction of **10** with $(CH_3CN)_3Cr(CO)_3$ further increased metal density of the polymers affording polysiloxanes **12** and **13** carrying ($\eta^5$-$C_5H_4$)Fe($\eta^5$-$C_5H_5$) and ($\eta^6$-$C_6H_5$)$Cr(CO)_3$ moieties hanging from their polysiloxane chain. Similar reactions, starting from 1,1,3,3-tetramethyldisiloxane and phenyltris(dimethylsiloxy)silane, were also a convenient way to prepare the corresponding homo and heterometallic model compounds [MePhFcSi$(CH_2)_2Me_2Si]_2O$ (**5**), [{($\eta^6$-$C_6H_5$)$Cr(CO)_3$}MeFcSi$(CH_2)_2Me_2Si]_2O$ (**6**), and PhSi[$OMe_2Si(CH_2)_2$MePhSiFc]$_3$ (**7**). These model compounds and the metallopolysiloxanes were characterized by IR, multinuclear NMR spectroscopies and mass spectrometry. Thermogravimetric analysis (TGA) established that dendronized polysiloxanes **9** and **11**, with ferrocenyl dendrons derived from **3**, possess higher thermal stability than parent ferrocenyl polysiloxanes **8** and **10**. Ferrocenyl dendronized polysiloxanes **9** and **11** yield ceramic products, which have been characterized by SEM and EDX microanalyses. Solution electrochemical studies showed that all the ferrocenyl units present in polysiloxanes **8**−**13** are electrochemically independent. Ferrocenyl polysiloxanes **8**−**11**, deposited electroactive films onto electrode surfaces. Their well-defined and persistent redox waves are characteristic of electrochemically stable, surface-confined reversible redox couples.

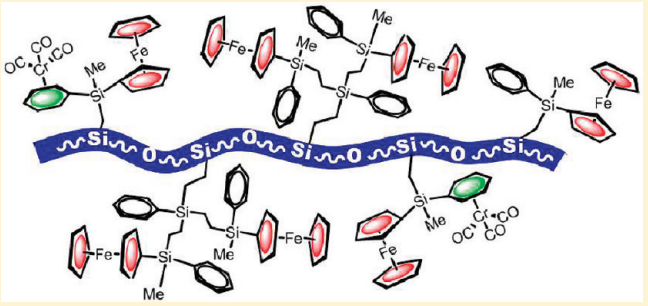

## INTRODUCTION

During the past 2 decades metal-containing polymers have attracted considerable scientific attention because of their unique geometries, physicochemical characteristics, and great potential as functional materials.[1−5] Among these metallopolymers, silicon-based ferrocenyl polymers were found to exhibit useful properties including redox and catalytic activity and magnetic and optical responses, as well as good thermal stability and solubility.[5−8] In addition, silicon-containing ferrocenyl polymers have significant applications as precursors to functional magnetic ceramics,[9] conducting materials,[10] and electrode modifiers[7,11] and also as electrochemical biosensors.[12]

A challenging synthetic target is the possibility to integrate different, selected, organometallic centers in predetermined sites of the silicon-based polymer structure. The presence of two or more, different metal centers within the same macromolecule can profoundly affect both the physical properties and the reactivity of the resulting polymeric system. Although synthetic methods for silicon-containing homometallic polymers are well developed,[6−8] synthetic efforts for the construction of silicon-based polymers having two or more different organotransition metal moieties are limited, and only a few attempts have been made in this direction so far. Manners et al. have reported interesting well-defined heterometallic polyferrocenylsilanes containing pendant cobalt, molybdenum and nickel organometallic units, which were prepared by complexation of the C≡C bonds of acetylide substituted polyferrocenylsilanes with $Co_2(CO)_8$, {Mo($\eta^5$-$C_5H_5$)$(CO)_2\}_2$, and {Ni($\eta^5$-$C_5H_5$)$(CO)\}_2$ units, respectively.[13] Very recently, the same group has also prepared remarkable examples of silicon-containing heterobimetallic block copolymers with ferrocene and cobaltocenium units in the main-chain by an appealing photocontrolled ring-opening polymerization process of strained sila-[1]ferrocenophane and cobaltocenophane monomers.[14] In addition to silicon-based heterometallic polymers, well-defined carbosilane dendrimers containing different organotransition metal moieties within the same dendritic molecule have also been synthesized.[15,16]

**Received:** July 28, 2011
**Revised:** September 8, 2011
**Published:** September 29, 2011

In the last years, we have been exploring routes for the construction of new families of redox-active organometallic dendritic and polymeric structures.[7,15,17] In this context, our long-standing interest in siloxane-based organometallic polymers and in silicon-based organometallic dendrimers, naturally led us to the investigation of novel dendronized polymers in which ferrocenyl-containing dendritic building-blocks are grafted onto multifunctional, flexible poly(methylsiloxane) backbones. Dendronized polymers merge concepts of dendrimers and linear polymers, as they are composed of a linear polymer backbone to which dendrons of increasing size (i.e., generations) are appended.[18] This exclusive architecture makes dendronized polymers unique macromolecules and interesting candidates for a variety of nanoscale applications, such as molecular wires, self-adaptative materials and functional scaffolds for catalysis.[18] The combination of the unique architectural features of dendritic molecules together with the electroactivity of the ferrocene entity and the well-known remarkable features and properties of poly(methylsiloxanes) (such as chemical stability, thermal and thermo-oxidative stability, dynamic flexibility, high permeability to gases and low toxicity),[19] is an attractive strategy for controlling the physical and redox properties of the resulting hybrid macromolecules. In spite of the fact that a variety of dendronized polymers has been synthesized and numerous metallodendrimers have been reported,[20] only very few studies have addressed the synthesis of dendronized polymers containing organotransition metallic moieties.[21] In this context, Manners and co-workers have reported noteworthy organometallic silicon-containing dendronized polymers, which were constructed by the macromolecular reaction of a reactive poly(ferrocenylchloromethylsilane) backbone and dendrons with a focal hydroxy group.[21a] Likewise, Astruc et al. have recently prepared interesting ferrocenyl-containing dendronized polymers by the AIBN-initiated radical polymerization of ferrocenyl-functionalized styrenic dendrons.[21b]

With these considerations in mind, as the first step toward developing ferrocenyl-containing dendronized polysiloxanes, some years ago we prepared polysiloxanes containing small pendant electroactive wedges possessing electronically communicated ferrocenyl moieties.[7a] In this work, we extend our effort in the area of siloxane-based redox-active organometallic macromolecules. Herein, we report full details on the synthesis via hydrosilylation chemistry, characterization, thermal behavior, and redox properties of a series of new polysiloxanes functionalized with small appended dendritic wedges containing both electron-donor ferrocenyl units and electron-acceptor ($\eta^6$-aryl)tricarbonylchromium fragments, and we compare their properties with those of closely related siloxane-bridged model compounds.

## RESULTS AND DISCUSSION

**Synthesis and Characterization of Siloxane-Bridged Model Compounds 5−7.** The synthesis of the targeted poly{ferrocenyl}-poly{($\eta^6$-$C_6H_5$)$Cr(CO)_3$} siloxane-based dendronized materials implies, as first step, the preparation of suitable olefin-substituted dendritic fragments with desired organometallic functionalities that will subsequently be grafted to Si−H-containing reactive polysiloxane backbones by means of hydrosilylation reactions. Hydrosilylation is one of the most important reactions to form Si−C bonds in organosilicon chemistry,[22] although its use for the introduction of organometallic moieties into macromolecular structures has been much less explored. Some noteworthy examples of ferrocenyl-containing silicon-based polymers prepared via hydrosilylation reactions have been reported by Pannell et al.,[8e,23a] Manners et al.,[23b] Sheridan et al.,[23c] Frey et al.,[8d] and Müller et al.[8i] and by our own group.[7a−d]

**Scheme 1. Synthesis of Si−Olefin and Si−Phenyl Bifunctionalized Ferrocenyl Compounds**

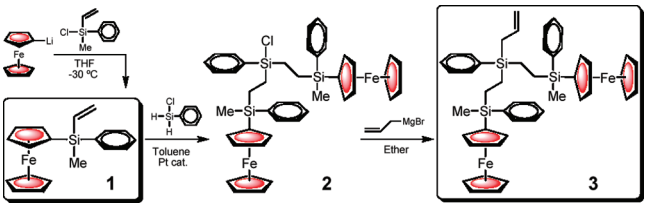


**Scheme 2. Synthetic Routes for the Preparation of Disiloxane Model Compounds 5 and 6**

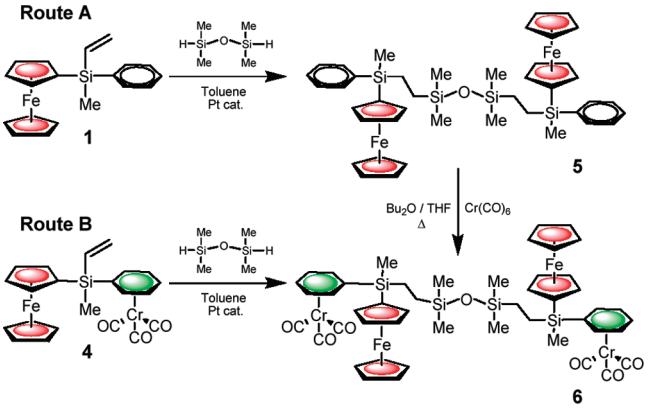


The key molecules from which we chose to construct homo and heterometallic polysiloxane materials were ferrocenylmethylphenylvinylsilane **1**, and first generation bis(ferrocenyl) dendron **3**. These starting molecules were successfully synthesized, as shown in Scheme 1, through the combination of several reactions, namely: (i) low temperature salt metathesis reaction between monolithioferrocene with methylphenylvinylchlorosilane, (ii) Karstedt's catalyzed hydrosilylation of **1** with phenylchlorosilane, and (iii) alkenylation reaction of the chlorosilane functionality of intermediate compound **2** with allylmagnesium bromide.[15a] Both ferrocenyl compounds, **1** and **3**, bear a single reactive focal C=C functionality, making further building of macromolecular structures by hydrosilylation possible, as well as additionally providing a phenyl binding site for potential coordination of a different organotransition metal fragment in addition to ferrocene.

Before preparing the targeted polysiloxanes bearing ferrocenyl and ($\eta^6$-aryl)$Cr(CO)_3$ moieties pendant to their backbones, well-defined siloxane-bridged homo and heterometallic model compounds were synthesized, in order to determine whether a similar strategy might provide access to heterometallic polysiloxanes and allow to understand the properties of this class of materials more thoroughly. In this way, the reactivity of the vinyl group in **1** toward a Si−H-difunctional disiloxane was, at first, studied as a model reaction, as it is outlined in Scheme 2. Hydrosilylation of **1** with 1,1,3,3-tetramethyldisiloxane, in toluene solution and in the presence of Karstedt's catalyst, occurred

**Scheme 3. Synthesis of T-Shaped Si−Phenyl Bearing Trisferrocenyl Compound 7**

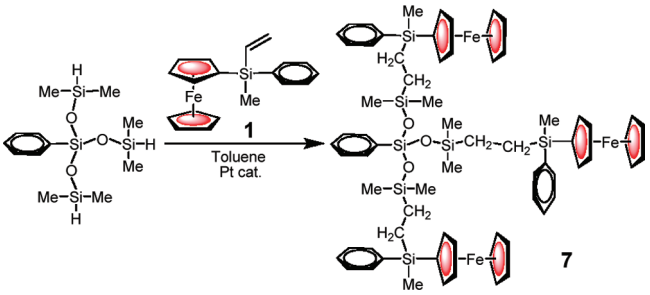


effectively with full conversion of the olefinic group after 4 h, at 45 °C. This reaction afforded the desired bimetallic **5**, containing silicon-bridged ferrocenyl and phenyl groups linked through the Si−O−Si chain. Purification of the resulting hydrosilylated product was effected by column chromatography on silica, resulting in bimetallic disiloxane-bridged model compound $[MePhFcSi(CH_2)_2Me_2Si]_2O$ (**5**) (Fc = $(\eta^5\text{-}C_5H_4)Fe(\eta^5\text{-}C_5H_5)$), which was isolated as an air stable, highly pure orange product, in 89% yield. $^1H$ and $^{13}C$ NMR spectral data of **5** (see below) suggested the regiospecific formation of the $\beta$-isomer since evidence for the formation of the $\alpha$-isomer was not detected.

For the synthesis of heterometallic model compound $[\{(\eta^6\text{-}C_6H_5)Cr(CO)_3\}MeFcSi(CH_2)_2Me_2Si]_2O$ (**6**) two synthetic approaches can be envisaged (paths A and B in Scheme 2). The first attempt to obtain **6** (path B, bottom) proceeded via hydrosilylation of the previously prepared vinylsilyl-functionalized heterobimetallic compound **4**[15a] with the bifunctional silylhydride, $[Me_2SiH]_2O$. In sharp contrast to ferrocenylmethylphenylvinylsilane **1**, all attempts to graft by hydrosilylation reaction, the $Cr(CO)_3$ complexed vinylsilane **4** failed in large measure, as only trace quantities of the desired heterometallic **6** were obtained. The poor reactivity of the Si−CH=$CH_2$ group in heterobimetallic **4**, as compared to the closely related homometallic **1**, in all probability reflects the presence of tricarbonylchromium fragment in **4**, which induced electron-deficiency in the phenyl rings bound to the Si−vinyl group and decreased the effectiveness of hydrosilylation with Si−H functionalized molecules.[24] In view of these results, for further synthetic studies, this path to **6** and related $Cr(CO)_3$-containing poly(methylsiloxanes) did not seem very promising and was therefore abandoned. The $\pi$-coordinating ability of the two electron-rich phenyl rings in **5** toward transition metals represented an alternative synthetic access to the targeted mixed ferrocenyl-chromium molecule **6** (Scheme 2, path A, top). For this purpose, we reacted bimetallic **5** with chromium hexacarbonyl in the donor medium *n*-dibutyl ether/THF, which after appropriate purification afforded the desired doubly $\eta^6$-complexed heterotetrametallic disiloxane **6** in reasonable yield.[25]

We were then interested in testing the hydrosilylation reactivity of vinylsilane **1** toward phenyltris(dimethylsiloxy)silane. The choice of this derivative was intentional since it contains three reactive Si−H groups that permit chemical modifications, and branched siloxane units, which make it a useful building block for the synthesis of more complex siloxy-type molecules. We have found that hydrosilylation of **1** with the trifunctional $PhSi[OSiMe_2H]_3$, under the same experimental conditions as those

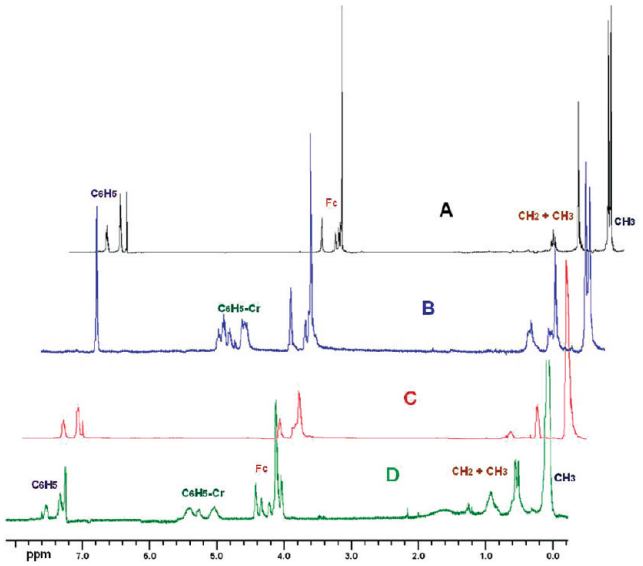


**Figure 1.** Comparison of the $^1H$ NMR spectra (in $CDCl_3$): (A) bisferrocenyl disiloxane model compound **5**; (B) heterometallic disiloxane model compound **6**; (C) ferrocenyl copolymer **8**; (D) $Cr(CO)_3$-containing ferrocenyl copolymer **12**.

used for the formation of **5**, was a successful process and afforded the hydrosilylated, T-shaped compound **7** (Scheme 3). Once separated, compound **7**, which contains three ferrocenyl moieties and four noncoordinated arene rings, was isolated as a crystalline yellow-orange solid. Freshly obtained, three-arm compound **7** was sufficiently soluble in $CH_2Cl_2$, THF, and $CDCl_3$, which enabled us to purify the compound by column chromatography, and to characterize it by IR and $^1H$, $^{13}C$ and $^{29}Si$ NMR spectroscopies and mass spectrometry (see below). However, the compound became insoluble after being dried during a long period under vacuum and stored during several weeks under argon, possibly due to the formation of supramolecular aggregates. Because of this insolubility, further reactions of trisferrocenyl derivative **7** with $Cr(CO)_6$, in order to obtain the corresponding heterometallic derivatives, are precluded.

The structural identities of novel siloxane-bridged compounds **5**−**7** were unambiguously supported by spectroscopic data and elemental analysis. The $^1H$ NMR spectra of **5**, **6**, and **7** revealed the formation of the desired products, as the integrated ratio of all different groups is in accord with the structural composition. All compounds show the pattern of resonances centered at about $\delta$ 4.0−4.1 and $\delta$ 4.1−4.5 ppm, characteristic of the unsubstituted and substituted cyclopentadienyl ligands in the ferrocenyl moieties.

In the $^1H$ NMR spectrum of heterometallic fully metalated disiloxane **6**, the complete $\eta^6$-coordination of the $Cr(CO)_3$ moieties to the two phenyl rings in **5** was confirmed by the absence of resonances in the range 7.3−7.5 ppm, in which the aryl resonances of noncoordinated **5** are observed, and by the existence of new signals of complexed arene protons between $\delta$ 5.1 and 5.5 ppm (see Figure 1, parts A and B). In addition, resonances at ca. ∼ 233 ppm due to the carbonyl carbon atoms were observed in the $^{13}C$ NMR spectra of **6**. For the doubly $\eta^6$-complexed heterotetrametallic compound **6**, additional evidence for coordination of the $Cr(CO)_3$ group to the phenyl rings included the presence of the two strong CO stretching vibrations at 1967 and 1889 $cm^{-1}$ in the IR spectra, related to the $A_1$ and E vibration modes of the $Cr(CO)_3$ tripod. Likewise, the IR spectra of **5**−**7**

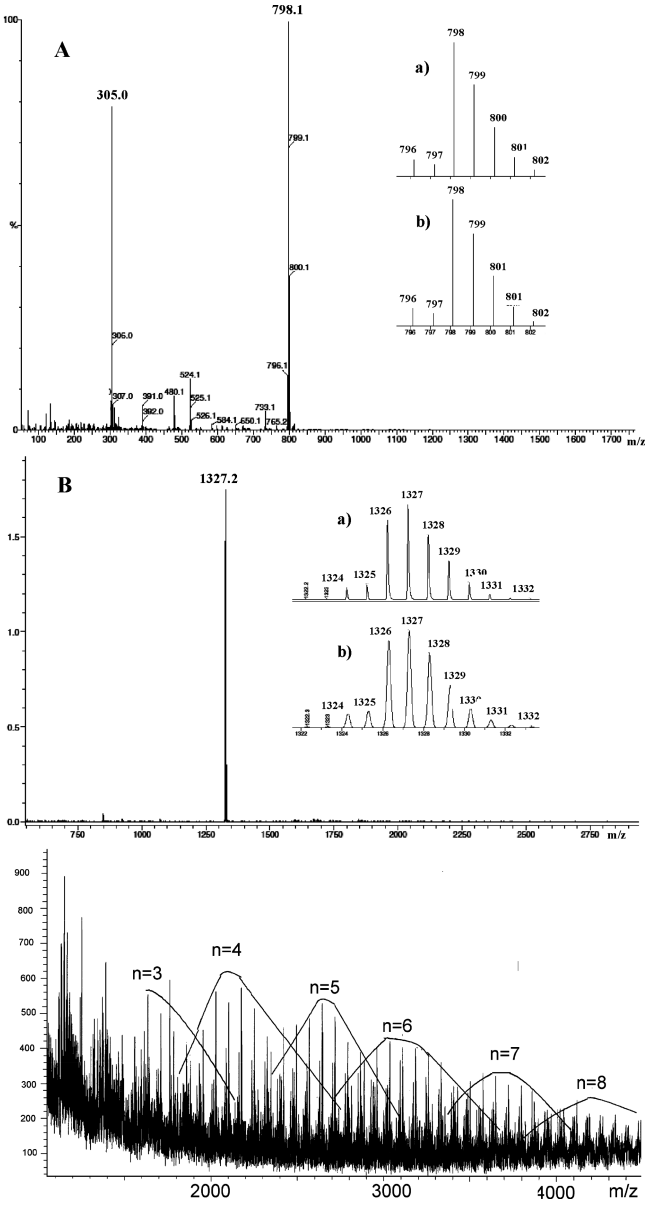


**Figure 2.** Mass spectra: (A) disiloxane model compound **5** (FAB); (B) tris(ferrocenyl)siloxane **7** (MALDI−TOF); (C) ferrocenyl dimethylsiloxane copolymer **8** (MALDI−TOF). The insets show the calculated (a) and experimental (b) isotopic patterns.

exhibit strong stretching vibrations, characteristic of Si−O−Si siloxane linkages near 1036−1132 $cm^{-1}$.

As expected, $^{29}Si$ NMR spectra of **5**−**7** exhibit two signals in each compound corresponding to two different types of silicon environments present in the molecules. The signals at $\delta = -5.1$ ppm (for **5**), −1.5 ppm (for **6**) and −5.3 ppm (for **7**) were assigned to the outer silicon atoms bridging the ferrocenyl and phenyl units, and the resonances shifted downfield at $\delta = 8.1$ ppm (for **5**), 8.3 ppm (for **6**), and 9.6 ppm (for **7**) were attributed to the inner D-type silicon atom in the Si−O−Si bridge. Trimetallic **7** exhibits an additional signal at $\delta = -77.7$ ppm characteristic of a trifunctional T silicon atom with a phenyl substituent.[26,27]

Mass spectrometry provided further evidence for the formation of the new polymetallic systems. Thus, fast atom bombardment (FAB) mass spectrum for bisferrocenyl disiloxane **5** gave the molecular ion at $m/z$ 798.1 as dominant peak, as well as some informative fragmentation peaks (Figure 2A). Likewise, in the FAB mass spectrum of **6**, peaks attributable to characteristic consecutive losses of $Cr(CO)_3$ and $2Cr(CO)_3$ units were detected, in addition to the peak corresponding to the molecular ion $M^+$ at $m/z$ 1069.9. Evidence of the targeted tris(ferrocenyl)-siloxane **7** was also provided by the MALDI−TOF mass spectrum (Figure 2B) which revealed a peak at $m/z = 1327.2$, corresponding to the molecular ion $M^+$. The insets in parts A and B of Figure 2 reveal that the agreement between the experimental and calculated isotopic patterns is excellent.

**Synthesis and Characterization of Homo- and Heterometallic Polysiloxanes 8−13.** The next task in the present study was to construct novel dendronized polymethylsiloxanes with both ferrocene and ($\eta^6$-aryl)tricarbonylchromium moieties, using the wedge-shaped dendritic fragments **1** and **3**. These starting ferrocenyl-containing derivatives bear a single reactive CH═$CH_2$ functionality to be grafted to the poly(hydrosiloxane) chains, without cross-linking during the grafting reaction. To this end, Karstedt-catalyzed reactions were carried out between the commercially available Si−H-polyfunctionalized copolymer $(Me_3SiO)(MeSiHO)_n(Me_2SiO)_m(SiMe_3)$ ($n$ = 30−35%, $m$ = 65−70%), and poly(methylhydrosiloxane), $(Me_3SiO)(MeSiHO)_n(SiMe_3)$ ($n \sim 35$), and the olefin-substituted compounds **1** and **3**, in toluene solutions (Scheme 4). Completion of these reactions was easily monitored by in situ $^1H$ NMR due to the disappearance of the Si−H resonance near $\delta$ 4.7 ppm, and IR spectroscopy by following the disappearance of the sharp $\nu$(Si−H) band, near 2170 $cm^{-1}$. These hydrosilylation reactions were not as facile as those occurred in the case of model compound **5** and thus, additional forcing conditions (temperatures around 100 °C and overnight reactions) were required to achieve complete conversion of the Si−H functionalities in the polysiloxane backbones.

Purification of resulting hydrosilylated polysiloxane products **8**−**11** was effected by repeated dissolutions of the reaction product in dichloromethane and precipitation in ethanol or hexane. The final compounds containing pendant dendritic side chains with ferrocenyl units linked to phenyl rings by a bridging silicon atom were isolated as air-stable orange-brown tacky oily materials which harden on standing. The obtained polysiloxanes **8**−**11** were soluble in common organic solvents such as THF, $CH_2Cl_2$, $CHCl_3$ and toluene. Dendronized polysiloxanes **9** and **11** form amber free-standing films when cast from dichloromethane or THF solutions.

Structural characterization of the ferrocenyl-containing dimethylsiloxane copolymers **8** and **9** and ferrocenyl homopolysiloxanes **10** and **11** was achieved by IR, $^1H$, $^{13}C$, and $^{29}Si$ NMR spectroscopies and MALDI−TOF mass spectroscopy. $^1H$ NMR spectra of **8**−**11** are similar to those of model compound **5**, but showing broad resonances (for the phenyl, ferrocenyl, methylene and methyl groups attached to silicon atoms), typical for polymers due to the slower motion of the protons. No unreacted Si−H bonds were present in polymers **8**−**11**, as indicated by $^1H$ NMR and IR spectroscopies suggesting full functionalization of the Si−H groups in the siloxane backbone (see, for instance, Figure 1C). In all cases $^1H$ and $^{13}C$ NMR spectroscopy of the hydrosilylated polysiloxanes show that the hydrosilylation reaction yields preferentially $\beta$ addition products although a negligible proportion of $\alpha$ addition products is observed in the case of ferrocenyl polysiloxane **9**. Two-dimensional heteronuclear NMR experiments have been used for the complete assignment of these polysiloxane systems. For instance, the {$^1H-^{29}Si$} HMBC

**Scheme 4. Synthetic Route to Polysiloxanes with Pendant Redox-Active Dendritic Wedges Containing Si-Bridged Ferrocenyl and Phenyl Units**

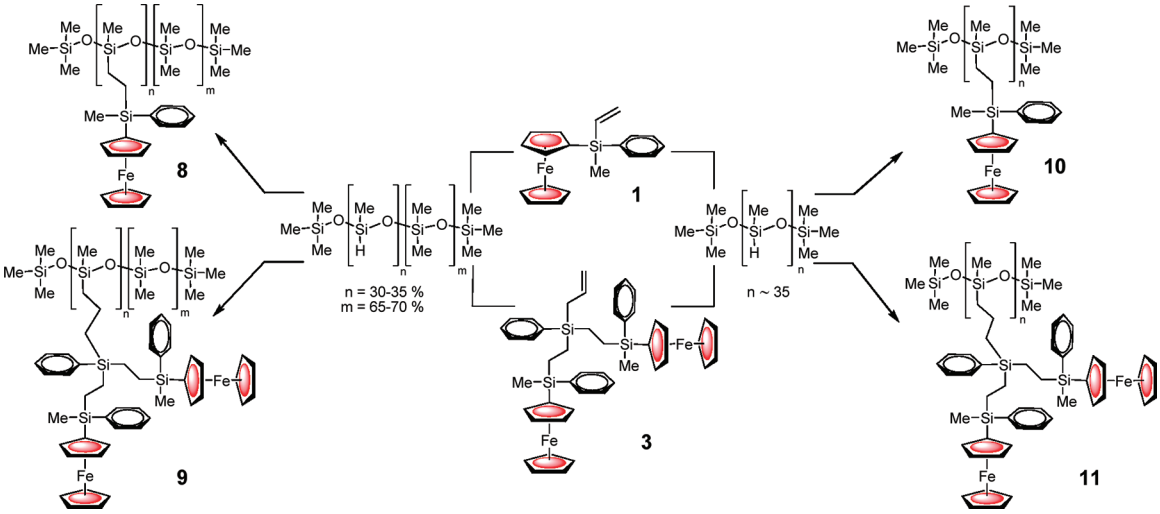


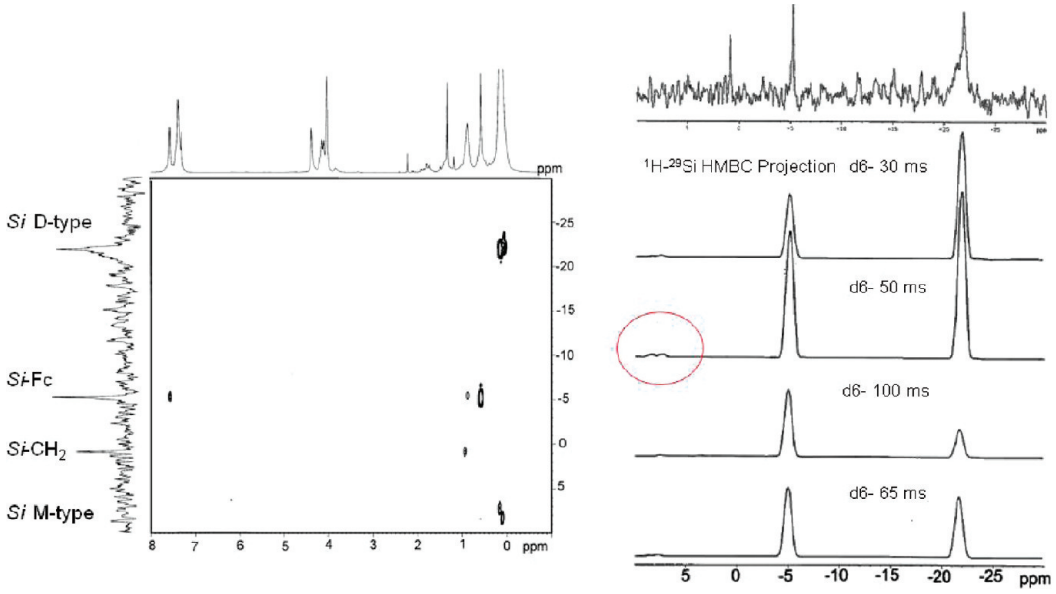


**Figure 3.** $\{^1H-^{29}Si\}$ HMBC spectrum ($CDCl_3$, 300 MHz) of **8** at $d$ = 50 ms (left). Projections of $\{^1H-^{29}Si\}$ HMBC experiments at different $d$ values (right).

(heteronuclear multiple-bond correlation), when setting the corresponding parameter according to the coupling constant ($d = {}^1/_2$ J), allows to identify the resonances of the minority silicon atoms. Particularly, in the case of the $\{^1H-^{29}Si\}$ HMBC spectrum of copolymer **8** (Figure 3), for an established value of $d$ = 50 ms that corresponds with a 7 Hz coupling constant, a resonance corresponding to minority, M-type, silicon nuclei near 9.0 ppm can be observed, corresponding to the $O-Si(CH_3)_3$ terminal units.[26] This peak does not appear in the monodimensional $^{29}Si$ NMR experiment, because these nuclei are in low proportion in the polymer chain. The resonances of the silicon atoms adjacent to ferrocenyl units, the D-type silicon atoms and the silicon attached to the $CH_2$ groups appeared in the expected regions.[27]

One of the most valuable tools for the characterization of polysiloxanes is MALDI−TOF, which provides a means to estimate molecular weight averages and molecular weight distributions and to determine the structure and terminal groups of a polymer sample.[28,29] The MALDI−TOF of copolymer **8** in the mass range below $m/z$ 5000 (Figure 2C) shows five major sets of peaks, each of them with a Gaussian shape, corresponding to oligomers that possess 4−8 organometallic wedges, pendant to the main Si−O−Si chain. In these sets, the peaks with the highest intensity are observed at $m/z$ 1634.5, 2026.5, 2640.5, 3106.7, 3646.7, and 4186.8. Each of these peaks is accompanied by several other peaks, equally spaced at 74 mass units apart, which corresponds to the mass of the $Me_2SiO$ repeat unit. The number-average molecular weight ($M_n$), the weight-average molecular

**Scheme 5. Synthetic Route to Polysiloxanes with Pendant Silicon-Bridged ($\eta^5$-$C_5H_4$)Fe($\eta^5$-$C_5H_5$) and ($\eta^6$-$C_6H_5$)$Cr(CO)_3$ Moieties**

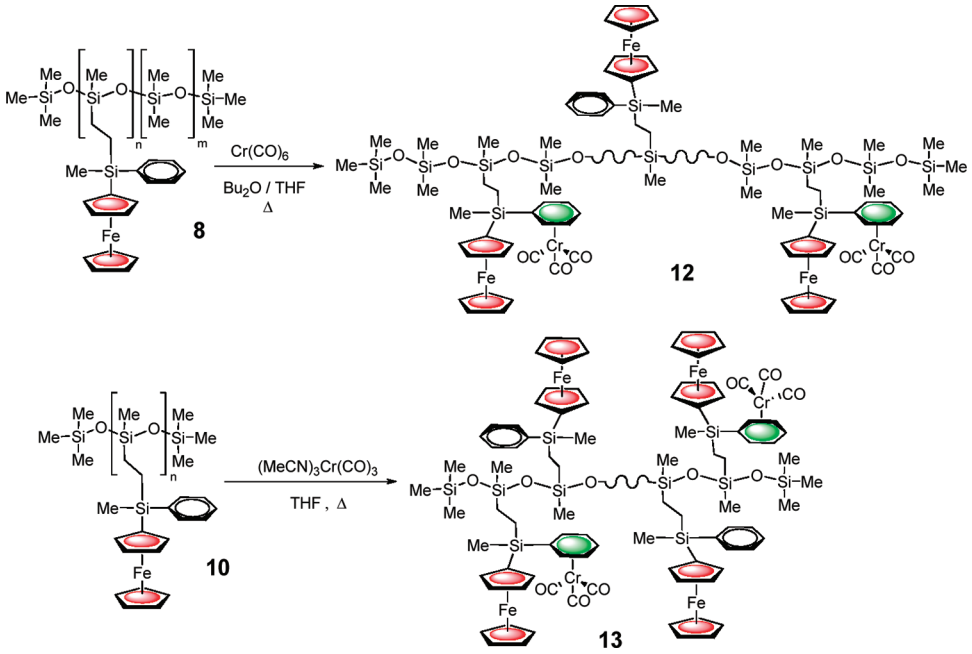


weight ($M_w$) and the PDI = $M_w/M_n$ can be derived from the MALDI−TOF,[28] resulting in values of $M_n$ = 2934.3, $M_w$ = 2950.9, and PDI ($M_w/M_n$) = 1.06. Although peaks at higher $m/z$ values are not observed in this spectrum, the existence of higher molecular weight species cannot be ruled out, since the MALDI−TOF technique tends to show considerable molecular weight discrimination for polydisperse samples.[29] Unfortunately, analysis of second generation dendronized polysiloxane **9** and of homopolysiloxanes **10** and **11** proved to be unsuccessful under all tested conditions.

In view of the heterometallic model compound **6** reaction results, for the synthesis of the novel siloxane-based poly-{ferrocenyl}-poly{($\eta^6$-$Cr(CO)_3$} dendronized molecules, we have used the route in which hydrosilylation of the Si−$CH{=}CH_2$ focal group with polyfunctional siloxane was performed before the coordination of phenyl ligands to $Cr(CO)_3$. Thermal treatment of parent copolymer **8** with $Cr(CO)_6$ afforded the heterometallic copolymer **12** (Scheme 5). The thermal displacement of CO in the $Cr(CO)_6$ by the phenyl rings of copolymer **8** was not as facile as with bimetallic model compound **5** and more forcing conditions (longer reaction times, about 96 h) were required in order to achieve a reasonable degree of $\eta^6$-coordination of the $Cr(CO)_3$ entity to the phenyl rings.

Figure 1 also shows the $^1$H NMR spectra of $Cr(CO)_3$−containing copolymer **12** (Figure 1D) and its precursor ferrocenyl copolymer **8** (Figure 1C), together with the $^1$H NMR spectra of disiloxane model compounds **5** and **6**. Similar to heterotetrametallic model **6**, in the $^1$H NMR spectrum of **12**, the aromatic proton peaks of the phenyl units $\eta^6$-coordinated to $Cr(CO)_3$ moieties appeared as a set of peaks around $\delta$ 5.0−5.6 ppm. In addition, resonances at around $\delta$ 7.3−7.6 ppm are observed corresponding to aromatic protons of the phenyl units noncomplexed to $Cr(CO)_3$ moieties. As determined by calculation from integration ratio of the protons of the complexed arene ring and those of the uncomplexed aryl moieties, copolymer **12** appears to consist approximately of 63% chromium-coordinated phenyl and of 37% uncoordinated phenyl units. In addition, in the IR spectra of $Cr(CO)_3$−containing copolymer **12**, very strong vibration bands typical of $\nu$(C≡O) carbonyl absorptions emerge at 1967 and 1890 $cm^{-1}$, which indicates that the integration of the $Cr(CO)_3$ metallic species into the Si−O−Si polymer structure has taken place.

Thermal synthetic procedure with $Cr(CO)_6$ has also been attempted for obtaining heterometallic homopolysiloxane **13** depicted in Scheme 5, using ferrocenyl homopolysiloxane **10** as precursor. Unfortunately, this method presented several problems because of the high temperatures and extremely long reaction periods, which apparently caused noticeable decomposition. Furthermore, NMR and MS data indicated that during the complexation reaction of the $Cr(CO)_3$ group to the phenyl rings, a competitive siloxane-chain scission reaction took place, resulting that the most highly $Cr(CO)_3$-complexed polysiloxanes were generated with a sacrifice in the molecular weight. Probably, the progressive degradation of the polysiloxane chain, during the course of the $Cr(CO)_3$-complexation reaction, was due to −Si−O−Si− chain scission caused by $Cr(CO)_6$ or a chromium containing material derived from it.[30] In addition, the formation of insoluble decomposition products made difficult the purification and characterization of this heterometallic product. These observations led us to try an alternative synthetic route, which involved synthesis of the derivative $(MeCN)_3Cr(CO)_3$ and subsequent reaction with polymer **10**. This method has an important advantage because the intermediate $(MeCN)_3Cr(CO)_3$ reacts at lower temperature with arene rings, thus avoiding possible cleavage of the polysiloxane backbone. In our hands, the direct reaction of a solution in THF of the tris(acetonitrile)crhomium derivative with another THF solution containing homopolymer **10** afforded the desired heterometallic homopolymer **13**


dx.doi.org/10.1021/ma201748d |*Macromolecules* 2011, 44, 7994–8007

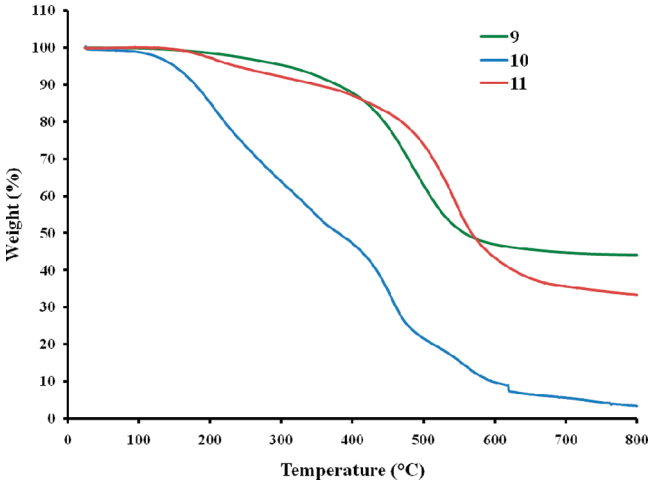


**Figure 4.** TGA thermograms of ferrocenyl polysiloxanes **9**, **10**, and **11** recorded under nitrogen at a heating rate of 10 °C $min^{-1}$.

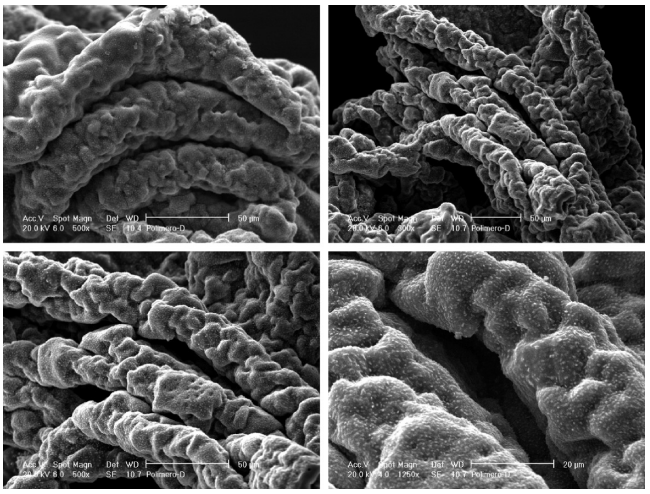

**Figure 5.** SEM micrographs of the ceramic material obtained by the pyrolysis of dendronized ferrocenyl polysiloxane **9**, at 1000 °C under a nitrogen atmosphere.

(Scheme 5), which shows in the IR spectrum the expected $\nu$(C≡O) bands at 1964 and 1885 $cm^{-1}$. In this case, $^1$H NMR spectroscopy indicated that polysiloxane **13** was constituted, approximately, of 65% $Cr(CO)_3$-coordinated phenyl units versus 35% uncoordinated phenyl groups. After the appropriate work-up, the desired heterometallic polysiloxanes **12** and **13** were isolated as yellowish tacky oils. Both products are air and moisture unstable and after several hours in solution yield a green residue, presumably as consequence of the Cr(0) centers oxidation.

**Thermal Stability of Ferrocenyl Dendronized Polysiloxanes.** The thermal properties of the ferrocene-containing polymethysiloxanes were evaluated by thermogravimetric analysis (TGA) under nitrogen. The thermal stability and degradation behavior of polysiloxanes **8**−**11** are strongly dependent on the size of the ferrocenyl-containing dendritic fragments appended to the siloxane backbone, as can be seen in Figure 4. Ferrocenylhomopolysiloxane **10**, in which each repeat unit bears pendant silicon-bridged ferrocenyl and phenyl units attached to the Si−O−Si main backbone, has a very low thermal stability. This polymer starts to lose mass even before 100 °C. Above this temperature, catastrophic decomposition occurs in several stages. The weight loss is continuous and takes place at a wide range of temperatures, which suggests a complex degradation process. By 515 °C, virtually only 20% of the initial sample weight remains. Thermal degradation of **10** resulted in almost complete polymer annihilation. In contrast, dendronized polysiloxanes **9** and **11**, both incorporating larger dendritic side chains derived from dendron **3**, are significantly more thermo-stable.

Dendronized homopoly(methylsiloxane) **11**, containing appended ferrocenyl-functionalized dendrons in all side chains, starts to lose its weight at a temperature above 200 °C (Figure 4) and shows a three-step thermolysis process. At 445 °C approximately only 17% of the initial weight of the sample is lost. The dendronized polysiloxane undergoes a rapid thermolytic degradation in the temperature region between 445−650 °C, after which the TGA curve is almost leveled off. By 650 °C, approximately 62% of the initial sample weight is lost. Little further weight loss is recorded when the sample is further heated to 800 °C. The ceramization yield of the polymer at this temperature is 35 wt %, much higher than of its related polysiloxane **10** under comparable pyrolysis conditions (∼5 wt %). This difference is reasonably associated with the difference in their molecular structures. Dimethylsiloxane copolymer **9**, with a lowest loading of pendant ferrocenyl-dendritic wedges, shows a single step smooth loss of mass, with onset of weight loss at 250 °C. By 380 °C only 10% of the initial sample weight is lost. The major weight loss of this dendronized polysiloxane occurs in the temperature region of 380−600 °C, after which the TGA curve is almost leveled off. No further weight loss is recorded when the sample is further heated to 800 °C, indicating that the polymer ceramizes by the high-temperature pyrolysis. Polymer **9** yielded 45% of ceramic residues. The higher ceramization yields of ferrocenyl dendronized polysiloxanes **9** and **11**, in comparison to that of its counterpart polysiloxane **10**, may be attributed to the higher stability of the highly branched metallopolysiloxane structure.[6e,31]

Since the TGA analyses showed that dendronized polysiloxanes **9** and **11**, functionalized with the largest ferrocenyl-dendritic wedges could be promising precursor candidates for ceramics, we further studied the residues obtained via their pyrolysis under a nitrogen stream at 1000 °C, by scanning electron microscopy (SEM) and energy-dispersive X-ray (EDX) microanalyses. The obtained ceramic products present magnetic properties and could be readily attracted to a magnet bar at room temperature. The clear images of the SEM micrographs indicate that the ceramic material is highly conductive. As shown in Figure 5, the ceramic produced by pyrolysis of ferrocenyl dendronized polysiloxane **9** is compact but rough in morphology. This ceramic material exhibits a regular structure comprising many three-dimensionally well-ordered thick cords, overlapping each other, whose surface is decorated with small clusters with sizes of a few hundred nanometers. This morphology is really curious because it seems that the pyrolyzed material retains the branched structure of the ferrocenyl dendronized polysiloxane chains, stacked on each other. We carried out EDX analyses to estimate the chemical compositions of the ceramic materials. For dendronized ferrocenylpolysiloxane **9**, EDX analyses in the bulk give a silicon:iron proportion of 13:1. In the clusters of the surface the contents change to a silicon:iron proportion of 3:1. This composition gradient of transition metal from the bulk to the surface suggests

**Table 1. Anodic Cyclic Voltammetric Data for Homo and Heterometallic Siloxane Compounds**[a]

| | Fe centered | | Cr centered |
|---|---|---|---|
| compound | $E_{1/2}$ (V)[b] | $E_{1/2}$ (V)[c] | $E$pa (V) |
| **1** | 0.44 [79] | | |
| **3** | 0.46 [83] | | |
| **4** | 0.50 [96] | | 0.97 |
| **5** | 0.46 [79] | | |
| **6** | 0.53 [95] | | 0.99 |
| **7** | 0.47 [127] | | |
| **8** | 0.47 [50] | 0.46 [9][c] | |
| **9** | 0.47 [59] | 0.45 [13][c] | |
| **10** | 0.45 [27] | 0.45 [5][c] | |
| **11** | 0.45 [97] | 0.43 [10][c] | |
| **12** | 0.53 [110] | | 0.93 |
| **13** | 0.50 [150] | | 0.92 |

[a] Measured in $CH_2Cl_2$ solution, scan rate $v$ = 0.1 V $s^{-1}$. [b] The peak potential separation values, $\Delta E_{peak}$ (mV), are indicated in brackets. [c] $E_{1/2}$ values corresponding to modified electrodes prepared by potential scanning in a solution of the corresponding ferrocenyl polysiloxane in 0.1 M $n$-$Bu_4NPF_6/CH_2Cl_2$ solution, and then transferred to a ferrocenyl polymer-free 0.1 M $n$-$Bu_4NPF_6/CH_2Cl_2$ solution.

that the ceramization process is accompanied by the formation of iron nanoclusters.

**Electrochemical Behavior of Disiloxane Model Compounds 5−7 and Ferrocenyl-Containing Polysiloxanes 8−13.** The anodic electrochemistry of ferrocenyl-functionalized siloxane-bridged model compounds **5**−**7** and ferrocenyl dendronized polysiloxanes **8**−**13** has been examined by cyclic voltammetry (CV) in dichloromethane solution containing tetra-*n*-butylammonium hexafluorophosphate ($n$-$Bu_4NPF_6$) as supporting electrolyte. The half-wave potentials ($E_{1/2}$) of the electrochemical processes are summarized in Table 1. The CV responses of disiloxanes **5** and **6** and polysiloxanes **8**−**10** and **12** are shown in Figures 6, 7 and 8, as representative examples.

The CV of model compound **5**, shown in Figure 6A, exhibits a single oxidation at $E_{1/2}$ = +0.46 V vs SCE. The voltammetric features ($i_{pc}/i_{pa}$ essentially equal to unit, $\Delta E_{peak}$ values about 70−100 mV and $E_{peak}$ independent of the scan rate) clearly show that oxidation of **5** is chemically and electrochemically reversible, resulting in the production of biferricinium disiloxane species $[\mathbf{5}^{2+}][PF_6^-]_2$. The fact that only a single oxidation wave was observed implies a simultaneous two-electron transfer at the same potential of the ferrocenyl subunits and indicates that the two ferrocenes in **5** behave independently,[32,33] as identical redox centers with no significant electronic communication between them through the disiloxane backbone.

Concerning **8**−**11**, these ferrocenyl-containing polysiloxanes were readily oxidized and reduced at platinum or glassy carbon electrode surfaces when dissolved in $CH_2Cl_2$ in the presence of the supporting electrolyte. As expected, the CVs of **8**−**11** (see, for example, Figure 6, parts B and C) showed a single reversible oxidation process associated with the one-electron oxidation of the pendant ferrocenyl groups. Some differences can be observed when comparing the cyclic voltammetric responses of model disiloxane **5** and ferrocenyl-containing polysiloxanes **8**−**11**. For biferrocenyl disiloxane **5** (Figure 6A), oxidation and reduction did not appear to affect the solubility of the molecule, so,

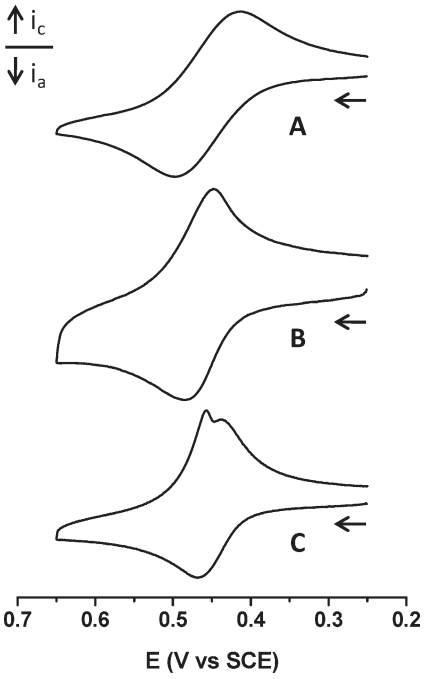


**Figure 6.** Cyclic voltammograms: (A) disiloxane model compound **5**; (B) ferrocenyl-polysiloxane **8**; (C) ferrocenyl dendronized polysiloxane **9** measured in $CH_2Cl_2$ solutions with 0.1 M $n$-$Bu_4NPF_6$ at a scan rate of 0.1 V $s^{-1}$.

voltammetric responses exhibited the wave shape characteristic of a freely diffusing soluble species undergoing reversible charge transfer. Thus, the oxidation of model compound **5** results in the production of the soluble, stable dicationic species $\mathbf{5}^{2+}$. As can be seen in Figure 6, parts B and C, the features of the voltammetric responses in dichloromethane solution of ferrocenyl-polysiloxanes **8**−**11** are somewhat different, since, whereas the anodic wave has a typical diffusional shape, a sharp cathodic wave was observed, which, in contrast, resembles more a surface wave. Consequently, for ferrocenyl polysiloxanes **8**−**11**, the use of the traditional $PF_6^-$ supporting electrolyte anion and low polarity dichloromethane solvent produces product surface interaction phenomena probably due to precipitation of oxidized polysiloxane species $\mathbf{8}^{n+}$, $\mathbf{9}^{n+}$, $\mathbf{10}^{n+}$, and $\mathbf{11}^{n+}$ (like their $PF_6^-$ salts) on the electrode surface, giving rise to distortions from the wave shape expected for reversible oxidation process. Reversal of the potential regenerates the soluble neutral ferrocenyl polysiloxanes. Similar adsorption-stripping voltammetric behavior has been observed previously in several examples of ferrocenyl-containing polymers,[34] including silicon-based ferrocenyl polymers[7,11] and polyvinylferrocene.[35] As expected, the solubility properties of these ferrocenyl-substituted polylsiloxanes **8**−**11** are also affected by the degree of ferrocene substitution. As the number of pendant ferrocenyl moieties per siloxane chain increases, the solubility of the polymer is more affected by the state of charge in the ferrocene units. Consequently, neutral fully ferrocene-substituted dendronized homopolysiloxanes **9** and **11** became the most insoluble upon oxidation and had the largest precipitation effects. It is interesting to note that the well-behaved cyclic voltammetric responses observed for dendronized polysiloxanes **9** and **11**, bearing ferrocenyl-functionalized pendant dendritic wedges, contrast with the electrochemical behavior of dendronized polyferrocenylsilanes synthesized by Manners et al.[21a] For these latter dendronized polymers, the steric bulkiness of the

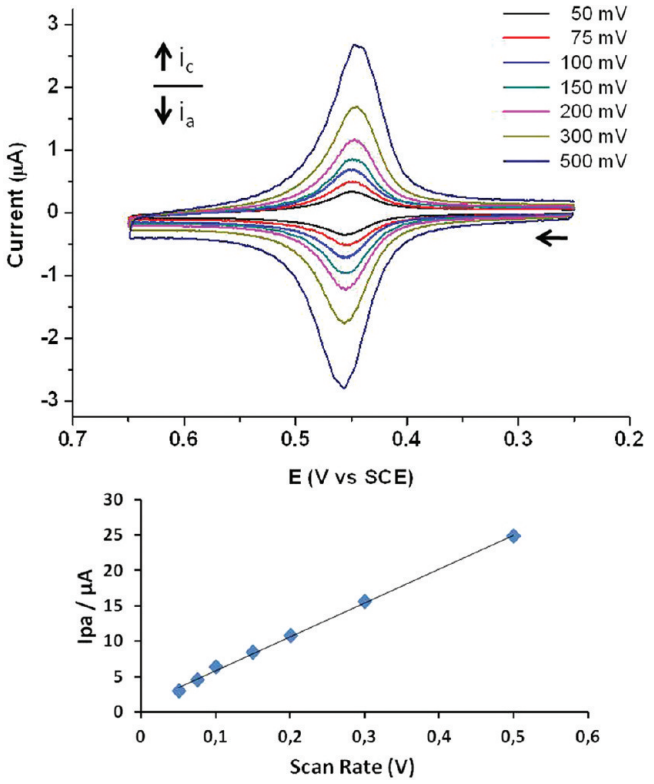


**Figure 7.** Cyclic voltammetric responses of a platinum-disk electrode modified with a film of ferrocenyl-containing polysiloxane **10**, measured in 0.1 M $Bu_4NPF_6/CH_2Cl_2$ at different potential scan rates (mV $s^{-1}$). Scan rate dependence upon the anodic peak current is shown.

large nonelectroactive dendrons attached around the ferrocene centers integrated in the main polymeric backbone leads to slower electron transfer reactions, resulting in poorly resolved cyclic voltammetric waves.

In addition, it is important to note the great ability of ferrocenyl polysiloxanes **8**−**11** to modify glassy-carbon and platinum electrodes, resulting in electroactive films of ferrocenyl polysiloxane materials that remains persistently attached to the electrode surface. The electrodeposition of the polymers can be carried out on Pt or glassy-carbon electrodes, either by controlled potential electrolysis (at ∼+0.5 V) or by repeated cycling (between +0.2 and +0.60 V vs SCE) in degassed $CH_2Cl_2$ solutions of electroactive polysiloxanes **8**−**11**. The electrochemical behavior of films of **8**−**11** was studied by CV in ferrocenyl-polysiloxanes-free $CH_2Cl_2$ solution containing only supporting electrolyte (*n*-$Bu_4NPF_6$). The voltammetric response of a film of polysiloxane **10** is shown in Figure 7 as a representative example. A well-defined symmetrical oxidation−reduction wave, corresponding to the ferrocene/ferricinium couple is observed, with a formal potential value $E_{1/2}$ = +0.45 V vs SCE which is identical to the formal potential of the ferrocenyl-polysiloxane in solution (Table 1). The wave shape is typical of a surface−confined reversible couple,[35−37] with the expected linear relationship of peak current to potential sweep rate, for values up to 500 mV $s^{-1}$. For the studied film shown in Figure 7, the peak to peak separation values ($\Delta E_{peak}$) vary from 2 mV at a scan rate of 25 mV $s^{-1}$, to 9 mV at 500 mV $s^{-1}$, which suggests that the rate of electron transfer is rapid on the time scale. In addition the full width at half-maximum ($E_{fwhm}$) of the surface voltammetric wave

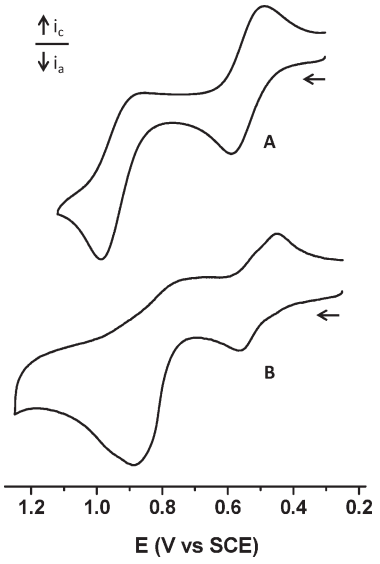


**Figure 8.** CV responses, in $CH_2Cl_2$ solutions with 0.1 M *n*-$Bu_4NPF_6$: (A) heterometallic disiloxane model compound **6**; (B) heterometallic polysiloxane **12** (measured at a scan rate of 0.1 V $s^{-1}$).

(about 60 mV, at a scan rate of 100 mV $s^{-1}$), suggests that there are no significant near neighbor interactions present between the ferrocenyl sites.[35] This behavior sharply contrasts with the redox response that we observed for multilayer films of related ferrocenyl polymers with backbones comprising cyclosiloxane moieties,[7b−d] which exhibit $E_{fwhm}$ values considerably narrower (typically $E_{fwhm}$ ∼ 5 mV) than ideally expected ($E_{fwhm}$ = 90.6 mV) for a one-electron transfer or for reactions of multiple, independent redox centers with identical formal potentials.[37,38] The stability of the ferrocenyl polysiloxane electroactive films was demonstrated by its nearly quantitative persistence after continuous CV scans in $CH_2Cl_2$/*n*-$Bu_4NPF_6$ solution. Likewise, after standing in air for several weeks, the redox response was practically unchanged without loss of electroactive material. The high stability of these surface confined polyferrocenylsiloxane films is an important observation since the applications of modified electrodes require extensive redox cycling.

As far as model compound **6** is concerned, the CV of this heterotetrametallic disiloxane molecule in the potential region between 0 and +1.10 V vs SCE (Figure 8A), proceeds in two well-resolved, diffusion controlled, oxidation processes at about $E_{1/2}$ = 0.53 V and $E_{pa}$= 0.99 V vs SCE, respectively, due to its two different redox sites. The first nearly reversible oxidation process is ascribed to the oxidation of the iron centers, and the second one to the oxidation of the chromium centers. The $E_{1/2}$ value of the first oxidation process is significantly higher than the $E_{1/2}$ found for oxidation of the iron centers of the related homobimetallic ferrocenyl precursor **5** (see Table 1) and this is reasonable, due to the electron-withdrawing nature of the adjacent ($\eta^6$-$C_6H_5$)$Cr(CO)_3$ moiety, bound trough a bridging silicon atom to the ferrocenyl units. Moreover, the chromium centered oxidation of heterometallic **6** shows a slight anodic shift with respect to the anodic potential of the unbound ($\eta^6$-benzene)tricarbonylchromium, ($\eta^6$-$C_6H_6$)$Cr(CO)_3$, ($E_{pa}$= 0.88 V vs SCE in $CH_2Cl_2$) as a result of the positive charges in $\mathbf{6}^{2+}$ generated after the first oxidation process. Similar to the model compound **6**, heterometallic polysiloxanes **12** and **13** displayed qualitatively similar CV responses (see Figure 8B and

Supporting Information), although in these cases the second anodic waves, corresponding to the oxidation of the pendant ($\eta^6$-$C_6H_5$)$Cr(CO)_3$ moieties, were considerably broadened and the redox process displayed electrochemical irreversibility, as shown by the absence of the corresponding cathodic peak in the reverse scan.

## CONCLUSIONS

Novel, highly functionalized polysiloxanes bearing small appended redox-active dendritic wedges, with electron-donor ferrocenyl units and electron-acceptor ($\eta^6$-aryl)tricarbonylchromium fragments, were synthesized. To this end, suitable ferrocenyl-dendritic wedges **1** and **3** containing a focal olefinic functionality were first constructed. Subsequently, these dendrons were grafted to Si−H-functionalized polysiloxane backbones, via hydrosilylation chemistry affording, successfully, methylsiloxane homo- and copolymers **8**−**11** bearing silicon-bridged ferrocenyl and phenyl pendant groups.

The novel ferrocenyl polysiloxanes are air and moisture-stable and soluble in common organic solvents. During the thermal treatment of $Cr(CO)_6$ with polysiloxane **10**, in which each repeat unit bears side chains with Si-bridged ($\eta^5$-$C_5H_4$)Fe($\eta^5$-$C_5H_5$) and $C_6H_5$ groups, the complexation of the pendant phenyl groups by $Cr(CO)_3$ was accompanied by a competing siloxane-chain scission process. TGA analysis showed that the thermal stability of the novel ferrocenyl polysiloxanes **8**−**11** strongly depends on the size of the ferrocenyl dendritic fragment appended to the siloxane backbones. Ferrocenyl dendronized polysiloxanes **9** and **11** are thermally stable to ca. 200−250 °C under $N_2$ (heating rate 10 °C $min^{-1}$) and at more elevated temperatures yield ceramic residues in relatively high amounts. Solution electrochemical studies showed that all the ferrocenyl redox units present in the ferrocenyl dendronized polysiloxanes are electrochemically independent. In addition, we have demonstrated the feasibility of modifying electrode surfaces with stable electroactive films of these siloxane-based polyferrocenyl dendronized molecules. Further extensions of this synthetic strategy are in progress with the aim to prepare highly ferrocenyl-functionalized dendronized polysiloxanes using dendrons of higher nuclearity.

## EXPERIMENTAL SECTION

**Materials.** All reactions and compound manipulations were performed in an oxygen- and moisture-free atmosphere ($N_2$ or Ar) using standard Schlenk techniques. Solvents were dried by standard procedures over the appropriate drying agents and distilled immediately prior to use. *n*-Dibutylether and toluene were distilled from sodium. Chromium hexacarbonyl and ferrocene (Aldrich) were purified by sublimation before use. Platinum-divinyltetramethyldisiloxane complex in xylene (3−3.5% Pt concentration) (Karstedt's catalyst) available from ABCR was used as received. Poly(methylhydrosiloxane) ($Me_3SiO$)-(MeSiHO)n($SiMe_3$) ($M_n$ 1700−3200, $n \sim 35$) and 1,1,3,3-tetramethyldisiloxane were obtained from Aldrich and used as received. Phenyltris-(dimethylsiloxy)silane and ($Me_3SiO$)$(MeSiHO)_n(Me_2SiO)_m(SiMe_3)$ ($n$ = 30−35%; $m$ = 65−70%, average $M_n$ 2000−2100) were purchased from ABCR. Tris(acetonitrile)tricarbonylchromium(0) was prepared by reaction of $Cr(CO)_6$ with acetonitrile overnight, according to the literature.[39] The vinyl-functionalized compounds ($CH_2$═CH)MePhSiFc (**1**) and ($CH_2$═$CHCH_2$)PhSi[$(CH_2)_2$MePhSiFc]$_2$ (**3**) were synthesized as we have previously described.[15a] Silica gel (70−230 mesh) (Merck) was used for column chromatographic purifications.

**Instrumentation.** Infrared spectra were recorded on Bomem MB-100 FT-IR and on Perkin-Elmer 100 FT-IR spectrometers. NMR spectra were recorded on Bruker-AMX-300 and Bruker DRX-500 spectrometers. Chemical shifts were reported in parts per million ($\delta$) with reference to residual solvents resonances for $^1$H and $^{13}$C NMR ($CDCl_3$, $^1$H, $\delta$ 7.27 ppm; $^{13}$C, $\delta$ 77.0 ppm; and $(CD_3)_2CO$, $^1$H, $\delta$ 2.09 ppm; $^{13}$C, $\delta$ 205.9 and 30.6 ppm). $^{29}$Si NMR spectra were recorded with inverse-gated proton decoupling in order to minimize nuclear Overhauser effects. FAB mass spectral analyses were conducted on a VG Auto Spec mass spectrometer equipped with a cesium ion gun. The MALDI−TOF mass spectra were obtained using a Reflex III (Bruker) mass spectrometer equipped with a nitrogen laser emitting at 337 nm. Dichloromethane solutions of the matrix (dithranol, 10 mg/mL) and dichloromethane or hexane solutions of the corresponding compound (1 mg/mL) were mixed in the ratio 20:5. Then, 0.5−1 $\mu$L of the mixture were deposited on the target plate using the dried droplet method. The positive ion and the reflectron mode were used for this analysis. The thermogravimetric analyses (TGA) of the samples were performed using a TGA Q-500 instrument coupled with an EGA oven. The measurements were carried out under $N_2$ (90 mL $min^{-1}$) with a heating rate of 10 °C $min^{-1}$. The morphology of the ceramic residues was investigated with scanning electron microscopy (SEM) using a Philips XL30 instrument coupled with an EDAX DX4i analyzer. Elemental analyses were performed by the Microanalytical Laboratory, SIDI, Universidad Autónoma de Madrid, Spain.

**Electrochemical Measurements.** Cyclic voltammetric experiments were recorded on a Bioanalytical Systems BASCV-50W potentiostat. $CH_2Cl_2$ (spectrograde) for electrochemical measurements was freshly distilled from calcium hydride under argon. The supporting electrolyte used was tetra-*n*-butylammonium hexafluorophosphate (Fluka), which was purified by recrystallization from ethanol and dried in vacuum at 60 °C. The supporting electrolyte concentration was typically 0.1 M. A conventional three-electrode cell connected to an atmosphere of prepurified nitrogen was used. All cyclic voltammetric experiments were performed using either a platinum-disk working electrode ($A$ = 0.020 $cm^2$) or a glassy carbon-disk working electrode ($A$ = 0.070 $cm^2$) (both Bioanalytical Systems), each of which were polished on a Buehler polishing cloth with Metadi II diamond paste, rinsed thoroughly with purified water and acetone, and dried. All potentials were referenced to the saturated calomel electrode (SCE). Under our conditions, the decamethylferrocene redox couple $[FeCp^*_2]^{0/+}$ is −0.056 V vs SCE in $CH_2Cl_2$/0.1 M *n*-$Bu_4NPF_6$. A coiled platinum wire was used as a counter electrode. Solutions were, typically, $10^{-3}$ M or $10^{-4}$ in the redox active species. The solutions for the electrochemical experiments were purged with nitrogen and kept under an inert atmosphere throughout the measurements. From the CVs of the modified electrodes, the surface coverage, $\Gamma$ (mol/$cm^2$) of the ferrocenyl sites were calculated from the charge, $Q$, under the voltammetric current peaks, using $\Gamma = Q/nFA$.[37]

**Synthesis of Ferrocenyl−Disiloxane Model Compound [MePhFcSi$(CH_2)_2$$Me_2$Si]$_2$O (5).** Under an argon atmosphere, a solution of 1,1,3,3-tetramethyldisiloxane (0.10 g, 0.75 mmol) in dry, freshly distilled toluene (5.0 mL) was added dropwise to a stirred solution of **1** (0.54 g, 1.63 mmol) in 30 mL of toluene containing 40 $\mu$L of Karstedt's catalyst (3−5% Pt, in xylene). The solution was stirred and heated to 45 °C. After 4 h, the completeness of the reaction was confirmed by the disappearance of the resonance corresponding to the Si−H proton in the $^1$H NMR spectrum ($\delta$ 4.7 ppm). After filtration, the solvent was removed under vacuum, affording an orange oily residue which was purified by column chromatography on silica using hexane as eluent. A first orange band containing the excess of **1** was collected and subsequently a major orange band afforded the desired hydrosilylated product **5**. After solvent removal, **5** was isolated as an orange air-stable solid. Yield: 0.53 g (89%). Anal. Calcd for $C_{42}H_{54}Si_4OFe_2$: C, 63.14; H,

6.82. Found: C, 63.42; H, 6.78. $^1$H NMR ($CDCl_3$, 300 MHz): $\delta$ 0.04 (s, 12H, OSi($CH_3$)$_2$), 0.52 (s, 6H, FcSi$CH_3$), 0.52, 0.89 (m, 8H, $CH_2$), 4.05 (s, 10H, $C_5H_5$), 4.09, 4.14, 4.35 (m, 8H, $C_5H_4$), 7.35, 7.54 (m, 10H, $C_6H_5$). $^{13}$C{$^1$H} NMR ($CDCl_3$, 125 MHz): $\delta$ −4.5 (FcSi$CH_3$), −0.2 (OSi($CH_3$)$_2$), 7.0, 10.7 ($CH_2$), 68.3 ($C_5H_5$), 69.3, 70.8, 71.0, 73.6 ($C_5H_4$), 127.7, 128.8, 134.1, 138.5 ($C_6H_5$). $^{29}$Si{$^1$H} NMR ($CDCl_3$, 99 MHz): $\delta$ −5.1 (FcSi$CH_3$), 8.1 (O$Si$($CH_3$)$_2$). IR: $\nu$(Si−O−Si) 1036−1131 cm$^{-1}$, $\nu$(Si−C) 788 cm$^{-1}$. MS (FAB): $m/z$ (%): 798.1 [M$^+$] (100), 305.0 [SiMe($C_6H_5$)Fc]$^+$ (82).

**Synthesis of Heterometallic Disiloxane Model [{($\eta^6$-$C_6H_5$)Cr(CO)$_3$}MeFcSi($CH_2$)$_2$Me$_2$Si]$_2$O (6).** In a 100 mL two-necked round-bottomed flask equipped with an air-cooled reflux condenser, argon inlet and magnetic stir bar, a degassed solution of 0.41 g (1.87 mmol) of Cr(CO)$_6$ and **5** (0.1 g, 0.12 mmol) in a mixture of 60 mL of *n*-dibutylether and THF (9/1, v/v) was heated at reflux temperature. The reaction was monitored by occasionally cooling a sample of the supernatant solution to room temperature and recording the IR and $^1$H NMR spectra. Over the course of the reaction, new carbonyl bands at 1967 and 1889 cm$^{-1}$ were observed to increase in intensity. Likewise in the $^1$H NMR ($CDCl_3$) spectrum, the resonances in the 7.3−7.5 ppm region progressively disappeared while new resonances in the range 5.1−5.5 were detected. After stirring for 24 h, the reaction mixture was cooled to +4 °C overnight. The greenish suspension was filtered through a pad of Celite to remove the small amounts of insoluble decomposition products and some unreacted solid Cr(CO)$_6$. From the resulting light orange solution, the solvent was removed under reduced pressure, affording a yellow solid which was purified by treatment with hexane solution at low temperature. After filtration and solvent elimination the desired tetrametallic **6** was isolated as a yellow-orange oil. Yield: 0.09 g (70%). Anal. Calcd for $C_{48}H_{54}Si_4O_7Fe_2Cr_2$: C, 53.83; H, 5.09. Found: C, 54.14; H, 5.20. $^1$H NMR ($CDCl_3$, 300 MHz): $\delta$ 0.07 (s, 12H, OSi($CH_3$)$_2$), 0.56 (s, 6H, FcSi$CH_3$), 0.65, 0.92 (m, 8H, $CH_2$), 4.13 (s, 10H, $C_5H_5$), 4.16, 4.21, 4.43 (m, 8H, $C_5H_4$), 5,13, 5.40, 5.48 (m, 10H, $C_6H_5$). $^{13}$C{$^1$H} NMR ($CDCl_3$, 125 MHz): $\delta$ −4.5 (FcSi$CH_3$), −0.2 (OSi($CH_3$)$_2$), 6.8, 10.7 ($CH_2$), 66.6, 68.4, 71.4, 71.5, 73.5, 73.7 ($C_5H_5$/$C_5H_4$), 90.2, 95.6, 99.9, 100.4 ($C_6H_5$), 233.2 (CO). $^{29}$Si{$^1$H} NMR ($CDCl_3$, 99 MHz): $\delta$ −1.5 (Fc$Si$$CH_3$), 8.3 (O$Si$($CH_3$)$_2$). IR: $\nu$(C≡O) 1967 and 1889 cm$^{-1}$, $\nu$(Si−O−Si) 1036−1132 cm$^{-1}$, $\nu$(Si−C) 789 cm$^{-1}$. MS (FAB): $m/z$ (%): 1069.9 [M$^+$] (18), 934.0 [M$^+$] − Cr(CO)$_3$ (27), 798.1 [M$^+$] − 2Cr(CO)$_3$ (35), 305.0 [SiMe($C_6H_5$)Fc]$^+$, (100).

**Synthesis of PhSi[OMe$_2$Si($CH_2$)$_2$MePhSiFc]$_3$ (7).** To a stirred solution of **1** (0.07 g, 0.21 mmol) in dry, freshly distilled toluene (5 mL) were added 10 $\mu$L of Karstedt's catalyst, under Ar atmosphere. The mixture was stirred at room temperature for 0.5 h. A solution of phenyltris(dimethylsiloxy)silane (0.02 g, 0.06 mmol) in dry toluene (5 mL) was added dropwise. The mixture was heated to 45−50 °C during 24 h. At this stage, $^1$H NMR spectroscopy confirmed the complete disappearance of the Si−H proton resonance of the starting hydrosilane. The reaction medium was then cooled to room temperature, filtered, concentrated under vacuum, and the remaining product was purified by column chromatography on silica gel using hexane as eluent. A first band containing excess of **1** was eluted and, subsequently, a second major orange band was collected with hexane/$CH_2Cl_2$ (10:2). Solvent removal afforded the desired trimetallic **7** as an air-stable, orange, solid. Yield: 0.06 g (75%). Anal. Calcd for $C_{69}H_{86}Si_7O_3Fe_3$: C, 62.49; H, 6.53. Found: C, 62.75; H, 6.61. $^1$H NMR ($(CD_3)_2CO$, 300 MHz): $\delta$ 0.13 (s, 18H, OSi($CH_3$)$_2$), 0.51 (s, 9H, FcSi$CH_3$), 0.59, 0.94 (m, 12H, $CH_2$), 4.04 (s, 15H, $C_5H_5$), 4.09, 4.14, 4.36 (m, 12H, $C_5H_4$), 7.35, 7.55 (m, 20H, $C_6H_5$). $^{13}$C{$^1$H} NMR ($(CD_3)_2CO$, 75 MHz): $\delta$ −4.3 (FcSi$CH_3$), −0.1 (OSi($CH_3$)$_2$), 7.7, 11.2 ($CH_2$), 69.0 ($C_5H_5$), 71.5, 71.7, 74.2, 74.3 ($C_5H_4$), 128.4, 129.6, 134.6, 134.9 ($C_6H_5$). $^{29}$Si{$^1$H} NMR ($(CD_3)_2CO$, 59 MHz): $\delta$ −77.7 (SiPh), −5.3 (FcSi$CH_3$), 9.6 (O$Si$($CH_3$)$_2$). IR: $\nu$(Si−O−Si) 1049−1131 cm$^{-1}$, $\nu$(Si−C) 788 cm$^{-1}$. MS (MALDI−TOF): $m/z$ 1327.2 [M$^+$].

**Synthesis of Ferrocenyl Dimethylsiloxane Copolymer 8.** To a solution of 0.18 g (0.56 mmol) of **1** in dry, freshly distilled toluene (20 mL) were added 40 $\mu$L of Karstedt's catalyst. Another solution of methylhydrosiloxane-dimethylsiloxane copolymer (Me$_3$SiO)(MeSiHO)$_n$-(Me$_2$SiO)$_m$(SiMe$_3$) ($n$ = 30−35%, $m$ = 65−70%), (0.10 g) in dry toluene (10 mL) was added dropwise. The reaction mixture was heated to 110 °C overnight. During this time the original orange color of the solution darkened to brown. After 24 h, the hydrosilylation reaction was found to be complete by IR and $^1$HNMR spectroscopies, as it was confirmed by the total disappearance of the Si−H band in the IR spectrum (2156 cm$^{-1}$) of the starting copolymer and of the resonance corresponding to the Si−H proton, near 4.7 ppm. The reaction mixture was then cooled to room temperature, filtered, and the solvent was removed under vacuum. The brown oily residue was dissolved in a small amount of $CH_2Cl_2$ and then precipitated in cold ethanol (three times) and dried under vacuum. Product **8** was obtained as a dark brown gum, soluble in $CH_2Cl_2$ and hexane. $^1$H NMR spectroscopy indicated full hydrosilylation of the Si−H bonds of the polysiloxane backbone. Yield: 0.21 g. $^1$H NMR ($CDCl_3$, 300 MHz): $\delta$ 0.06−0.09 (br, OSi($CH_3$)$_3$, OSi($CH_3$)$_2$, OSi($CH_3$)), 0.52 (br, $CH_2$, FcSi$CH_3$), 0.90 (m, $CH_2$), 4.04 (s, $C_5H_5$), 4.08, 4.13, 4.33 (m, $C_5H_4$), 7.32, 7.53 (m, $C_6H_5$). $^{13}$C{$^1$H} NMR ($CDCl_3$, 75 MHz): $\delta$ −4.5 (FcSi$CH_3$), −1.2 (OSi($CH_3$)$_2$), 1.0, 1.2, 1.8 (OSi$CH_3$), 6.7, 9.7 ($CH_2$), 68.2 ($C_5H_5$), 69.0, 70.7, 70.9, 73.5 ($C_5H_4$), 127.6, 128.8, 134.0, 138.2 ($C_6H_5$). $^{29}$Si{$^1$H} NMR ($CDCl_3$, 59 MHz): $\delta$ −20.0 (O$Si$($CH_3$)$_2$), −5.0 (FcSi$CH_3$), 0.9 (O$Si$$CH_2$), 9.0 (O$Si$($CH_3$)$_3$). IR: $\nu$(Si−O−Si) 1024−1105 cm$^{-1}$, $\nu$(Si−C) 800 cm$^{-1}$. MS (MALDI−TOF): $M_n$ = 2934.3, $M_w$ = 2950.9, polydispersity index $M_w/M_n$ = 1.01.

**Synthesis of Ferrocenyl Dendronized Dimethylsiloxane Copolymer 9.** Using the same method as detailed for the preparation of model compound **5** and copolymer **8**, ferrocenyl dendronized copolymer **9** was synthesized starting from copolymer ((Me$_3$SiO)-(MeSiHO)$_n$(Me$_2$SiO)$_m$(SiMe$_3$) ($n$ = 30−35%, $m$ = 65−70%), (0.04 g), ferrocenyl dendron **3** (0.19 g, 0.23 mmol) and 40 $\mu$L of Karstedt's catalyst in dry, freshly distilled, toluene (30 mL). After 18 h at 80 °C the $^1$H NMR spectroscopy confirmed the complete disappearance of the Si−H proton resonance of the starting copolymer. The reaction mixture was treated as above, and after the appropriate work-up, the resulting orange-brown tacky residue was dissolved in $CH_2Cl_2$ and precipitated in cold ethanol (three times). The ferrocenyl dendronized copolymer **9** was obtained as an orange-brown viscous product. $^1$H NMR spectroscopy indicated full hydrosilylation of the Si−H bonds of the polysiloxane backbone. Yield: 0.03 g. $^1$H NMR ($CDCl_3$, 300 MHz): $\delta$ 0.07−0.09 (br, OSi($CH_3$)$_3$, OSi($CH_3$)$_2$, OSi$CH_3$), 0.50 (br, $CH_2CH_2$, Fc−Si−$CH_3$), 0.80−0.90 (br, $CH_2CH_2CH_2$), 3.97 (s, $C_5H_5$), 4.04, 4.08, 4.31 (m, $C_5H_4$), 7.32, 7.50 (m, $C_6H_5$). $^{13}$C{$^1$H} NMR ($CDCl_3$, 125 MHz): $\delta$ −4.6 (FcSi$CH_3$), −0.3 (OSi($CH_3$)$_2$), 1.2 (OSi$CH_3$), 4.1, 7.7 ($CH_2CH_2$), 16.4, 17.7, 22.5 ($CH_2CH_2CH_2$), 68.3 ($C_5H_5$), 69.0, 70.8, 73.5, 73.6 ($C_5H_4$), 127.7, 128.9, 134.1, 134.3, 138.3 ($C_6H_5$). $^{29}$Si{$^1$H} NMR ($CDCl_3$, 99 MHz): $\delta$ −21.9 (O$Si$($CH_3$)$_2$), −5.2 (Fc$Si$$CH_3$), −1.0 ($Si$Ph), 0.9 (O−$Si$−$CH_2$). IR: $\nu$(Si−O−Si) 1022−1103 cm$^{-1}$, $\nu$(Si−C) 801 cm$^{-1}$.

**Synthesis of Ferrocenyl Homopolysiloxane 10.** This homopolymer was prepared in a similar manner as ferrocenyl polysiloxanes **8** starting from 0.32 g (0.96 mmol) of **1**, 0.05 g of poly(methylhydrosiloxane) ((Me$_3$SiO)(MeSiHO)$_n$(SiMe$_3$), $n$ ∼ 35) and 40 $\mu$L of Karstedt's catalyst. After 18 h at 90 °C, the reaction mixture was filtered and the solvent was removed under vacuum. The resulting orange-brown residue was dissolved in $CH_2Cl_2$ and precipitated with hexane twice. Ferrocenyl polysiloxane **10** was isolated as a brown gum. $^1$H NMR spectroscopy indicated full hydrosilylation of the Si−H bonds of the polysiloxane backbone. $M_n$ (g/mol): 13 900 (calculated according to a

polymerization degree of 35). Yield: 0.28 g. $^1$H NMR ($CDCl_3$, 300 MHz): $\delta$ 0.01 (br, OSi($CH_3$)$_3$, OSi$CH_3$), 0.45 (s, FcSi$CH_3$), 0.45, 0.88 (br, $CH_2$), 3.98 (br, $C_5H_5/C_5H_4$), 4.27 (br, $C_5H_4$), 7.28, 7.51 (m, $C_6H_5$). $^{13}$C{$^1$H} NMR ($CDCl_3$, 125 MHz): $\delta$ −4.4 (FcSi$CH_3$), −0.7 (OSi$CH_3$), 7.2, 9.9 ($CH_2$), 68.3, 68.9, 70.8, 71.0, 73.6 ($C_5H_5/C_5H_4$), 127.7, 128.9, 134.1, 138.1 ($C_6H_5$). $^{29}$Si{$^1$H} NMR ($CDCl_3$, 99 MHz): $\delta$ −22.4 (OSi$CH_3$), −5.0 (Fc*Si*$CH_3$). IR: $\nu$(Si−O−Si) 1033−1104 cm$^{-1}$, $\nu$(Si−C) 777 cm$^{-1}$.

**Synthesis of Ferrocenyl Dendronized Polysiloxane 11.** To a solution of ferrocenyl dendron **3** (0.02 g, 0.024 mmol) in toluene (2 mL) were added 40 $\mu$L of Karstedt's catalyst and another toluene solution containing 1.3 × $10^{-3}$ g of poly(methylhydrosiloxane) ((Me$_3$SiO)(MeSiHO)$_n$(SiMe$_3$), $n \sim 35$). The mixture was refluxed overnight. After filtration and remove the solvent the resulting orange-brown residue was dissolved in $CH_2Cl_2$ and precipitated with cold hexane several times. The desired ferrocenyl dendronized homopolysiloxane **11** was isolated as a dark gum. $^1$H NMR spectroscopy indicates full hydrosilylation of the Si−H bonds of the polysiloxane backbone. $M_n$ (g/mol): 30700 (calculated according to a polymerization degree of 35). Yield: 0.19 g. $^1$H NMR ($CDCl_3$, 300 MHz): $\delta$ 0.14 (br, OSi($CH_3$)$_3$, OSi$CH_3$), 0.58 (br, $CH_2CH_2$, FcSi$CH_3$), 0.87 (br, $CH_2CH_2CH_2$), 4.04 (br, $C_5H_4$), 4.11, 4.15, 4.38 (br, $C_5H_5$), 7.39, 7.57 (m, $C_6H_5$). $^{13}$C{$^1$H} NMR ($CDCl_3$, 125 MHz): $\delta$ −4.5 (FcSi$CH_3$), 1.9 (OSi$CH_3$), 4.0, 7.6 ($CH_2CH_2$), 14.2, 17.5, 22.8 ($CH_2CH_2CH_2$), 68.2 ($C_5H_5$), 68.5, 70.8, 71.0, 73.7 ($C_5H_4$), 127.9, 129.0, 134.0, 134.4, 137.2 ($C_6H_5$). $^{29}$Si{$^1$H} NMR ($CDCl_3$, 99 MHz): $\delta$ −22.1 (O*Si*$CH_3$), −5.1 (Fc*Si*$CH_3$), −1.3 (*Si*Ph). IR: $\nu$(Si−O−Si) 1023−1093 cm$^{-1}$, $\nu$(Si−C) 799 cm$^{-1}$.

**Synthesis of Heterometallic Dimethylsiloxane Copolymer 12.** In a 100 mL two-necked round-bottomed flask equipped with an air-cooled reflux condenser, argon inlet and magnetic stir bar, a degassed solution of 0.40 g (1.82 mmol) of chromium hexacarbonyl and 0.10 g of copolymer **8** in a mixture of 50 mL of *n*-dibutyl ether and THF (9:1, v:v) was heated to reflux temperature. The progress of the reaction was monitored by occasionally cooling a sample of the mixture to room temperature and recording the IR and $^1$H NMR spectra of the supernatant solution. After 96 h, and after checking by $^1$H NMR that further $\pi$-coordination of Cr(CO)$_3$ units to pendant phenyl rings was not longer possible, the greenish suspension was then cooled to room temperature and subsequently filtered through a pad of Celite to remove insoluble decomposition products. From the resulting yellow solution, the solvent was removed under vacuum. The obtained residue was purified by dissolving it in $CH_2Cl_2$ and by subsequent precipitation with hexane at low temperature. The desired heterometallic copolymer **12** was isolated as an air-unstable, yellow-orange oily product. Integration ratio of the protons of the Cr(CO)$_3$-complexed $C_6H_5$ rings and those of the uncomplexed $C_6H_5$ units, indicated that **12** consists on approximately 63% chromium-coordinated phenyl and 37% uncoordinated phenyl units. Yield: 0.20 g. $^1$H NMR ($CDCl_3$, 300 MHz): $\delta$ 0.08 (br, OSi($CH_3$)$_3$, OSi($CH_3$)$_2$, OSi$CH_3$), 0.52−0.56 (br, $CH_2$, FcSi$CH_3$), 0.93 (m, $CH_2$), 4.05, 4.12, 4.21, 4.34, 4.42 (m, $C_5H_5/C_5H_4$), 5.04, 5.28, 5.59 (Cr−$C_6H_5$), 7.33, 7.54, (m, $C_6H_5$). IR: $\nu$(C≡O) 1967 and 1890 cm$^{-1}$, $\nu$(Si−O−Si) 1018−1103 cm$^{-1}$, $\nu$(Si−C) 798 cm$^{-1}$.

**Synthesis of Heterometallic Polysiloxane 13.** Recently prepared (MeCN)$_3$Cr(CO)$_3$ (0.5 g, 1.93 mmol) was dissolved in dry, freshly distilled, oxygen-free THF and treated with a THF solution of ferrocenyl polysiloxane **10** (0.10 g) under argon. The stirred mixture was heated gently to reflux with IR and $^1$H NMR monitoring of the course of the reaction. After 48 h the mixture was cooled to room temperature and filtered through a short column of Celite. From the yellow filtrate the solvent was removed under vacuum and the yellowish residue was purified in a similar manner as the heterometallic copolymer **12**. The integration ratio of the protons of the Cr(CO)$_3$-complexed $C_6H_5$ rings and those of the uncomplexed $C_6H_5$ units indicated that **13** consists of approximately of 65% chromium-coordinated phenyl and 35% uncoordinated phenyl units. Yield: 0.15 g. $^1$H NMR ($CDCl_3$, 300 MHz): $\delta$ 0.06−0.12 (br, OSi($CH_3$)$_3$, OSi$CH_3$), 0.56, 1.00 (br, FcSi$CH_3$), 1.00−1.60 (m, $CH_2$), 4.05, 4.13, 4.21, 4.35, 4.42 (m, $C_5H_5/C_5H_4$), 5.07, 5.31, 5.40, 5.48 (Cr−$C_6H_5$), 7.35, 7.55, (m, $C_6H_5$). IR: $\nu$(C≡O) 1964 and 1885 cm$^{-1}$, $\nu$(Si−O−Si) 1023−1097 cm$^{-1}$, $\nu$(Si−C) 798 cm$^{-1}$.

## ■ ASSOCIATED CONTENT

**Supporting Information.** Structural characterization data (IR, NMR and mass spectra), additional CVs for **5**−**13**, and energy-dispersive X-ray (EDX) analyses of ceramic residues. This material is available free of charge via the Internet at http://pubs.acs.org.

## ■ AUTHOR INFORMATION

**Corresponding Author**
*E-mail: isabel.cuadrado@uam.es.

## ■ ACKNOWLEDGMENT

We gratefully acknowledge the financial support provided by the Spanish Ministerio de Ciencia e Innovación, Project CTQ2009-09125/BQU. S.B. acknowledges the Ministerio de Educación y Ciencia for a FPU grant. We would like to thank valuable assistance and helpful discussions of Dr. E. Salvador and Dr. M. J. de la Mata on SEM and TGA techniques, respectively, and Dr. M. Alonso and Dr. M. L. Gallego on MALDI techniques.

## ■ REFERENCES

(1) Manners, I. *Synthetic Metal-Containing Polymers*; Manners, I., Ed.; Wiley-VCH: Weinheim, Germany, 2004.

(2) *Macromolecules Containing Metal and Metal-Like Elements. Transition Metal-Containing Polymers*; Abd-El-Aziz, A. S., Carraher, C. E., Jr., Pittman, C. U., Sheats, J. E., Zeldin, M., Eds.; Wiley-Interscience: Hoboken, NJ, 2006.

(3) *Frontiers in Transition Metal-Containing Polymers*; Abd-El-Aziz, A. S., Manners, I., Eds.; Wiley-Interscience: Hoboken, NJ, 2007.

(4) *Metal-Containing and Metallosupramolecular Polymers and Materials*; Schubert, U. S., Newkome, G. R., Manners, I., Eds.; Vol. 928, ACS: Washington DC, 2006.

(5) For leading reviews on ferrocene-containing polymers, see: (a) Nguyen, P.; Gómez-Elipe, P.; Manners, I. *Chem. Rev.* **1999**, *99*, 1515–1548.(b) Peckham, T. J.; Gómez-Elipe, P.; Manners, I. In *Metallocenes. Synthesis, Reactivity, Applications*, Togni, A., Halterman, R. L., Eds.; Wiley-VCH: New York, 1998; pp 723−771. (c) Pittman, C. U. *J. Inorg. Organomet. Polym* **2005**, *15*, 33–55.(d) Long, N. J.; Kowalski, K. In *Ferrocenes. Ligands Materials and Biomolecules*; Stępnicka, P., Ed.; John Wiley & Sons: West Sussex, U.K., 2008, Chapter 10, pp 393−446. (e) Bellas, V.; Rehahn, M. *Angew. Chem., Int. Ed.* **2007**, *46*, 5082–5104. (f) Abd-El-Aziz, A. S.; Manners, I. *J. Inorg. Organomet. Polym.* **2005**, *15*, 157–195. (g) Bellas, V.; Rehahn, M. *Angew. Chem., Int. Ed.* **2007**, *46*, 5082–5104. (h) Whittell, G. R.; Manners, I. *Adv. Mater.* **2007**, *19*, 3439–3468.

(6) (a) Foucher, D. A.; Tang, B. Z.; Manners, I. *J. Am. Chem. Soc.* **1992**, *114*, 6246–6247. (b) Foucher, D. A.; Ziembinski, R.; Tang, B. Z.; Macdonald, P. M.; Massey, J.; Jaeger, R.; Vancso, G. J.; Manners, I. *Macromolecules* **1993**, *26*, 2878–2884. (c) Pannell, K. H.; Dementiev, V. V.; Li, H.; Cervantes-Lee, F.; Nguyen, M. T.; Diaz, A. F. *Organometallics* **1994**, *13*, 3644–3650. (d) Dementiev, V. V.; Cervantes-Lee, F.; Parkanyi, L.; Sharma, H.; Pannell, K. H.; Nguyen, M. T.; Diaz, A. F. *Organometallics* **1993**, *12*, 1983–1987. (e) Sun, Q.; Xu, K.; Peng, H.; Zheng, R.; Häussler, M.; Tang, B. Z. *Macromolecules* **2003**, *36*, 2309–2320. (f) Masson, G.; Beyer, P.; Cyr, P. W.; Lough, A. J.; Manners, I. *Macromolecules* **2006**, *39*, 3720–3730.

(7) (a) Alonso, B.; González, B.; Ramírez, E.; Zamora, M.; Casado, C. M.; Cuadrado, I. *J. Organomet. Chem.* **2001**, *637*−*639*, 642–652. (b) Casado, C. M.; Cuadrado, I.; Morán, M.; Alonso, B.; Lobete, F.; Losada, J. *Organometallics* **1995**, *14*, 2618–2620. (c) Morán, M.; Casado, C. M.; Cuadrado, I.; Losada, J. *Organometallics* **1993**, *12*, 4327–4333. (d) Casado, C. M.; Cuadrado, I.; Morán, M.; Alonso, B.; Barranco, M.; Losada, J. *Appl. Organomet. Chem.* **1999**, *13*, 245–259. (e) Casado, C. M.; Morán, M.; Losada, J.; Cuadrado, I. *Inorg. Chem.* **1995**, *34*, 1668–1680.

(8) For recent examples of ferrocene-containing silicon-based polymers see, for example:(a) Soto, A. P.; Manners, I. *Macromolecules* **2009**, *42*, 40–42. (b) Miles, D.; Ward, J.; Foucher, D. A. *Macromolecules* **2010**, *42*, 9199–9203. (c) Miles, D.; Ward, J.; Foucher, D. A. *Organometallics* **2010**, *29*, 1057–1060. (d) Wurm, F.; Hilf, S.; Frey, H. *Chem.—Eur. J.* **2009**, *15*, 9068–9077. (e) Kumar, M.; Pannell, K. H. *J. Inorg. Organomet. Polym.* **2008**, *18*, 131–142. (f) Kumar, M.; Metta-Magana, A. J.; Pannell, K. H. *Organometallics* **2008**, *27*, 6457–6463. (g) McDowell, J. J.; Zacharia, N. S.; Puzzo, D.; Manners, I.; Ozin, G. A. *J. Am. Chem. Soc.* **2010**, *132*, 3236–3237. (h) Smith, G. S.; Patra, S. K.; Vanderark, L.; Saithong, S.; Charmant, J. P. H.; Manners, I. *Macromol. Chem. Phys.* **2010**, *211*, 303–312. (i) Kong, J.; Schmalz, T.; Motz, G.; Müller, A. E. H. *Macromolecules* **2011**, *44*, 1280–1291. (j) Eloi, J.-C.; Rider, D. A.; Cambridge, G.; Whittell, G. R.; Winnik, M. A.; Manners, I. *J. Am. Chem. Soc.* **2011**, *133*, 8903–8913.

(9) See, for example:(a) MacLachlan, M. J.; Ginzburg, M.; Coombs, N.; Coyle, T. W.; Raju, N. P.; Greedan, J. E.; Ozin, G. A.; Manners, I. *Science* **2000**, *287*, 1460–1463. (b) Liu, K.; Clendenning, S. B.; Friebe, L.; Chan, W. Y.; Zhu, X.; Freeman, M. R.; Yang, G. C.; Yip, C. M.; Grozea, D.; Lu, .; Manners, I. *Chem. Mater.* **2006**, *18*, 2591–2601. (c) Friebe, L.; Liu, K.; Obermeier, B.; Petrov, S.; Dube, P.; Manners, I. *Chem. Mater.* **2007**, *19*, 2630–2640. (d) Liu, K.; Fournier-Bidoz.; Ozin, G. A.; Manners, I. *Chem. Mater.* **2009**, *21*, 1781–1783.

(10) See, for example:(a) Resendes, R.; Nelson, J. M.; Fischer, A.; Jakle, F.; Bartole, A.; Lough, A. J.; Manners, I. *J. Am. Chem. Soc.* **2001**, *123*, 2116–2126. (b) Kulbaba, K.; Cheng, A.; Bartole, A.; Greenberg, S.; Resendes, R.; Coombs, N.; Safa-Sefat, A.; Greedan, J. E.; Stoever, H. D. H.; Ozin, G. A.; Manners, I. *J. Am. Chem. Soc.* **2002**, *124*, 12522–12534. (c) Espada, L.; Pannell, K. H.; Papkov, V.; Leites, L.; Bukalov, S.; Suzdalev, I.; Tanaka, M.; Hayashi, T. *Organometallics* **2002**, *21*, 3758–3761. (d) Papkov, V. S.; Gerasimov, M. V.; Dubovik, I. I.; Sharma, S.; Dementiev, V. V.; Pannell, K. H. *Macromolecules* **2000**, *33*, 7107–7115. (e) Pannell, K. H.; Imshennik, V. I.; Maksimov, Yu. V.; Ilina, M. N.; Sharma, H. K.; Papkov, V. S.; Suzdalev, I. P. *Chem. Mater.* **2005**, *17*, 1844–1850.

(11) (a) Nguyen, M. T.; Diaz, A. F.; Dementiev, V. V.; Pannel, K. H. *Chem. Mater.* **1993**, *5*, 1389–1394. (b) Huo, J.; Wang, L.; Yu, H.; Deng, L.; Ding, J.; Tan, Q.; Liu, Q.; Xiao, A.; Ren, G. *J. Phys. Chem. B* **2008**, *112*, 11490–11497See also ref 17.

(12) (a) Losada, J.; Armada, M . P. G.; Cuadrado, I.; Alonso, B.; Gonzalez, B.; Casado, C. M.; Zhang, J. *J. Organomet. Chem.* **2004**, *689*, 2799–2807. (b) Armada, M. P. G.; Losada, J.; Cuadrado, I.; Alonso, B.; Gonzalez, B.; Casado, C. M. *Electroanalysis* **2003**, *15*, 1109–1114.

(13) (a) Chan, W. Y.; Clendenning, S. B.; Berenbaum, A.; Lough, A. J.; Aouba, S.; Ruda, H. R.; Manners, I. *J. Am. Chem. Soc.* **2005**, *127*, 1765–1772. (b) Berenbaum, A.; Ginzburg-Margau, M.; Coombs, N.; Lough, A. J.; Safa-Sefat, A.; Greedan, J. E.; Ozin, G. A.; Manners, I. *Adv. Mater.* **2003**, *15*, 51–55.

(14) Gilroy, J. B.; Patra, S. K.; Mitchels, J. M.; Winnik, M. A.; Manners., I. *Angew. Chem., Int. Ed.* **2011**, *50*, 5851–5855.

(15) (a) Zamora, M.; Alonso, B.; Pastor, C.; Cuadrado, I. *Organometallics* **2007**, *26*, 5153–5164. (b) García, B.; Casado, C. M.; Cuadrado, I.; Alonso, B.; Morán, M.; Losada, J. *Organometallics* **1999**, *18*, 2349–2356.

(16) (a) Angurell, I.; Rossell, O.; Seco, M.; Ruiz, E. *Organometallics* **2005**, *24*, 6365–6373. (b) Angurell, I.; Lima, J. C.; Rodriguez, L.-I.; Rossell, O.; Seco, M. *New J. Chem.* **2006**, *30*, 1004–1008. (c) Benito, M.; Rossell, O.; Seco, M.; Segalés, G. *Organometallics* **1999**, *18*, 5191–5193. (d) Angurell, I.; Rossell, O.; Seco, M. *Chem.—Eur. J.* **2009**, *15*, 2932–2940. (e) Nievas, A.; Medel, M.; Hernández, E.; Delgado, E.; Martín, A.; Casado, C. M.; Alonso, B. *Organometallics* **2010**, *29*, 4291–4297.

(17) (a) Cuadrado, I. In *Silicon-Containing Dendritic Polymers*; Dvornic, P., Owen, M. J., Eds.; Springer: Berlin, 2009; pp 141−196. (b) Bruña, S.; Gonzlez-Vadillo, A. M.; Nieto, D.; Pastor, C.; Cuadrado, I. *Organometallics* **2010**, *29*, 2796–2807. (c) Cuadrado, I.; Casado, C. M. C.; Alonso, B.; Morán, M.; Losada, J.; Belsky, V. *J. Am. Chem. Soc.* **1997**, *119*, 7613–7614. (d) Casado, C. M.; González, B.; Cuadrado, I.; Alonso, B.; Morán, M.; Losada, J. *Angew. Chem., Int. Ed.* **2000**, *39*, 2135–2138. (e) Cuadrado, I.; Morán, M.; Casado, C. M.; Alonso, B.; Lobete, F.; García, B.; Ibisate, M.; Losada, J. *Organometallics* **1996**, *15*, 5278–5280. (f) Alonso, B.; Cuadrado, I.; Morán, M.; Losada, J. *J. Chem. Soc., Chem. Commun.* **1994**, 2575–2576. (g) Alonso, B.; Morán, M.; Casado, C. M.; Lobete, F.; Losada, J.; Cuadrado, I. *Chem. Mater.* **1995**, *7*, 1440–1443. (h) Castro, R.; Cuadrado, I.; Alonso, B.; Casado, C. M.; Morán, M.; Kaifer, A. E. *J. Am. Chem. Soc.* **1997**, *119*, 5760–5761. (i) Nieto, D.; González-Vadillo, A. M.; Bruña, S.; Pastor, C.; Kaifer, A. E.; Cuadrado, I. *Chem. Commun.* **2011**, *47*, 10398–10400.

(18) For excellent reviews on dendronized polymers see, for example: (a) Schlüter, A. D. *Top. Curr. Chem.* **2005**, *245*, 151–191. (b) Schlüter, A. D. *Top. Curr. Chem.* **1998**, *197*, 165–191. (b) Schlüter, A. D.; Rabe, J. P. *Ange. Chem. Int. Ed.* **2000**, *39*, 864–883. (c) Frauenrath, H. *Prog. Polym. Sci.* **2005**, *30*, 325–384. (d) Hawker, C. J.; Wooley, K. L. *Science* **2005**, *309*, 1200–1205.

(19) (a) Noll, W. *Chemistry and Technology of Silicones*; Academic Press: New York, 1968. (b) *Inorganic Polymers*, Mark, J. E., Allcock, H. R., West, R., Eds.; Oxford University Press: Oxford, U.K., 2005, Chapter 4, pp 154−199. (c) Brook, M. A. *Silicon in Organic, Organometallic, and Polymer Chemistry*; Wiley: New York, 2000; pp 256−308.

(20) For reviews on organometallic dendrimers, see for example: (a) Cuadrado, I.; Morán, M.; Casado, C. M.; Alonso, B.; Losada, J. *Coord. Chem. Rev.* **1999**, *193*−*195*, 395–445. (b) Hearshaw, M. A.; Moss, J. R. *Chem. Commun.* **1999**, 1–8. (c) Rossell, O.; Seco, M.; Angurell, I. *C. R. Chim.* **2003**, *6*, 803–817. (d) Chase, P. A.; van Koten, G. *J. Organomet. Chem.* **2004**, *689*, 4016–4054.(d) Hwang, S.-H.; Newkome, G. R. In *Frontiers in Transition Metal-Containing Polymers*; Abd-El-Aziz, A. S., Manners, I., Eds.; Wiley-Interscience: Hoboken, NJ, 2007; Chapter 10, pp 399−438. (e) Astruc, D.; Ornelas, C.; Ruiz, J. *Acc. Chem. Res.* **2008**, *41*, 841–856.

(21) For interesting examples of dendronized polymers containing organotransition metal moieties, see:(a) Kim, K. T.; Han, J.; Ryu, C. Y.; Sun, F. C.; Sheiko, S. S.; Winnik, M. A.; Manners, I. *Macromolecules* **2006**, *39*, 7922–7930. (b) Boisselier, E.; Shun., A. C. K.; Ruiz, J.; Cloutet, E.; Belin, C.; Astruc, D. *New J. Chem.* **2009**, *33*, 246–253. (c) Suijkerbuijk, B. M. J. M.; Shu, L.; Gebbink, R. J. M. K.; Schlüter, A. D.; van Koten, G. *Organometallics* **2003**, *22*, 4175–4177.

(22) (a) *Hydrosilylation. A Comprehensive Review on Recent Advances. Advances in Silicon Science*, Vol. 1; Marciniec, B., Ed.; Springer Science: Berlin, 2009. (b) *Comprehensive Handbook on Hydrosilylation*; Marciniec, B., Ed.; Pergamon Press: Oxford, U.K., 1992. (c) Ojima, I. In *The Chemistry of Organic Silicon Compounds*; Patai, S., Rappoport, Z., Eds.; John Wiley & Sons: New York, 1989; Part 2, pp 1479−1526.

(23) (a) Kumar, M.; Pannell, K. H. *J. Inorg. Organomet. Polym.* **2007**, *17*, 105–110. (b) Hilf, S.; Cyr, P. W.; Rider, D. A.; Manners, I.; Ishida, T.; Chujo, Y. *Macromol. Rapid Commun.* **2005**, *26*, 950–954. (c) Jain, R.; Lalancette, R. A.; Sheridan, J. B. *Organometallics* **2005**, *24*, 1458–1467.

(24) It is well-known that electron-withdrawing substituents on the silicon atom of the Si-vinyl group decrease the rate of hydrosilylation processes compared to the more electron-donating groups.

(25) For recent examples of related $Cr(CO)_3$-containing phenylsilyl derivatives, see,Sharma, H. K.; Cervantes-Lee, F.; Pannell, K. H. *J. Organomet. Chem.* **2010**, *695*, 1168–1174.

(26) (a) *The Analytical Chemistry of Silicones*; Smith, A. L., Ed; John Whiley & Sons, Inc.: New York, 1991; p 347−414. (b) Williams, E. A. In *The Chemistry of Organic Silicon Compounds*; Vol 1, Part 1, Patai, S., Rappoport, Z., Eds.; JohnWiley & Sons: New York, 1989; pp 511−550. (c) Schraml, J. In *The Chemistry of Organic Silicon Compounds*; Vol. 3,

Rappoport, Z., Apeloig, Y., Eds.; JohnWiley & Sons: New York, 2001; pp 223−339.

(27) The symbols, M, D. and T represent framework silicon atoms which possess, 3 ($R_3Si-O$), 2 ($-O-R_2Si-O$) and 1 ($-O-RSi(-O)_2$) organyl substituents, respectively.

(28) Montaudo, G.; Montaudo, M. S.; Puglisi, C.; Samperi, F. *Rapid Commun. Mass Spectrom.* **1995**, *9*, 1158–1163.

(29) Nielen, M. W. F. *Mass. Spec. Rev.* **1999**, *18*, 309–344.

(30) Although polymethylsiloxanes are molecular structures with pronounced thermal and thermo-oxidative stability, it is also well established that the thermal degradation of these polymeric chains is a very complex process that can occur through different mechanisms and is sensitive to different factors such as the presence of certain solvents, residual transition metal and ionic impurities. For excellent leading reviews on the thermal stability of polysiloxanes see:(a) Dvornic, P. R. In *Silicon-Containing Polymers. The Science and Technology of Their Synthesis and Applications*, Jones, R. G.; Ando, W.; Chojnowski, J., Eds.; Kluwer Academic Publishers: Dordrecht, The Netherlands, Boston, MA, and London, 2000; pp 185−212. (b) Dvornic, P. R. In *Silicon Compounds: Silanes and Silicones*: Gelest Catalog, Gelest, Inc.: Arles, B., Larson, G., Eds; ABCR: Morrisville, PA, 2008; pp 441−454.

(31) (a) Shi, J.; Tong, B.; Li, Z.; Shen, J.; Zhao, W.; Fu, H.; Zhi, J.; Dong, Y.; Häussler, M.; Lam, J. W. Y.; Tang, B. Z. *Macromolecules* **2007**, *40*, 8195–8204. (b) Sun, Q.; Lam, J. W. Y.; Xu, K.; Xu, H.; Cha, J. A. K.; Wong, P. C. L.; Wen, G. W.; Zhang, X.; Jing, X.; Wang, F.; Tang, B. Z. *Chem. Mater.* **2000**, *12*, 2617–2624.

(32) Flanagan, J. B.; Margel, S.; Bard, A. J.; Anson, F. C. *J. Am. Chem. Soc.* **1978**, *100*, 4248–4253.

(33) Zanello, P. In *Inorganic Electrochemistry. Theory, Practice and Application*; Zanello, P., Ed.; Royal Society of Chemistry: Cambridge, MA, 2003.

(34) See, for example:(a) Albagli, D.; Bazan, G.; Wrighton, M. S.; Schrock, R. R. *J. Am. Chem. Soc.* **1992**, *114*, 4150–4158. (b) Albagli, D.; Bazan, G. C.; Schrock, R. R.; Wrighton, M. S. *J. Am. Chem. Soc.* **1993**, *115*, 7328–7334. (b) Crumbliss, A. L.; Cooke, D.; Castillo, J.; Wisian-Neilson, P. *Inorg. Chem.* **1993**, *32*, 6088–6094. (c) D'Silva, C.; Afeworki, S.; Parri, O. L.; Baker, P. K.; Underhill, A. *J. Mater. Chem.* **1992**, *2*, 225–230. (d) Nafady, A.; Mc. Adam, C. J.; Bond, A. M.; Moratti, S. C.; Simpson, J. *J. Solid State Electrochem.* **2009**, *13*, 1511–1519.

(35) (a) Merz, A.; Bard, A. J. *Am. Chem. Soc.* **1978**, *100*, 3222–3223. (b) Peerce, P. J.; Bard, A. J. *J. Electroanal. Chem.* **1980**, *112*, 97–115.

(36) Bard, A. J.; Faulkner, L. R. *Electrochemical Methods: Fundamentals and Applications*, 2nd ed.; Wiley: New York, 2001.

(37) (a) Murray, R. W. In *Molecular Design of Electrode Surfaces*; Murray, R. W., Ed.; Wiley: New York, 1992; p 1. (b) Abruña, H. D. In *Electroresponsive Molecular and Polymeric Systems*; Skotheim, T. A., Ed.; Dekker: New York, 1988; Vol. 1, p 97.

(38) In surface-immobilized redox species, the full-width-half-maximum ($E_{fwhm}$) for an ideal voltammetric surface wave is $E_{fwhm}$ = 90.6 mV. See refs 36 and 37.

(39) Santi, S.; Ceccon, A.; Bisello, A.; Durante, C.; Ganis, P.; Orian, L. *Organometallics* **2005**, *24*, 4691–4694.